

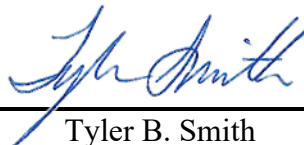
AN ABSTRACT OF THE THESIS OF

Joseph Townsend for the degree of Master of Science in Marine and Environmental Sciences presented on 26 November, 2019

Title: Lesion recovery of two reef-building coral species across shallow to mesophotic depths.

Following major stress events such as storms, disease outbreaks, or bleaching events, surviving corals must regenerate tissue in order to recover. We aimed to understand how this recovery changes from shallow to mesophotic depths, hypothesizing that deeper corals would regenerate more slowly and that this may limit resilience to storms and other acute stressors. Two species of reef building coral, *Orbicella franksi* (an intermediate-depth species) and *Agaricia lamarcki* (a depth-generalist), were tagged at selected sites across their overlapping depth range of 13 to 41m and directly monitored for recovery rate from experimentally generated lesions across time. Overall, recovery rates were distinct between species and across depths, with *O. franksi*, recovery rates showing high variability and declining at depth, behaving significantly different from *A. lamarcki*, the depth generalist. *A. lamarcki* maintained similar rates of recovery across the examined depth range, suggesting that it can attenuate its biology with changing light resources to maintain healing abilities in different environments. Recovery rates were additionally compared against environmental parameters such as temperature and wave energy, as well as against biological parameters such as colony size, lesion shape, and dominant endosymbiont type to understand their impact on recovery. While *A. lamarcki* recovery was not affected by changes in depth, temperature, or wave energy, *O. franksi* recovery was affected by depth, wave energy, and temperature variability. Collectively, this suggests that some mesophotic coral reefs, despite having high coral cover, may be slower to recover from stress events if dominated by non-depth generalist species, such as *O. franksi*, resulting in increased vulnerability to repeated stress events.

Abstract approved



Tyler B. Smith

©Copyright by Joseph Townsend
11/26/2019
All Rights Reserved

Lesion recovery of reef-building coral species across shallow to mesophotic depths

by
Joseph Townsend

A THESIS

Submitted to the
University of the Virgin Islands

In partial fulfillment of the requirements for the degree of

Master of Science

Presented 26 November, 2019
Commencement May 2020

Masters of Science thesis of Joseph Townsend presented on 11/26/2017

APPROVED:

DocuSigned by:



Tyler B. Smith

DocuSigned by:



Marilyn E. Brandt

DocuSigned by:



Monica Medina

DocuSigned by:



Sonaljit Mukherjee

DocuSigned by:



Lorraine Buckley, MMES Program

DocuSigned by:

Michelle Peterson

Michelle Peterson, College of Science and Mathematics

I understand that my thesis will become part of the permanent collection of the University of the Virgin Island Library. My signature below authorizes release of my thesis to any reader upon request

DocuSigned by:



Joseph Townsend

ACKNOWLEDGEMENTS

Thanks and gratitude to my committee, Dr. Marilyn Brandt, Dr. Monica Medina, Dr. Sonaljit Mukherjee, and my advisor Dr. Tyler Smith for patience, insight, and guidance in this project from its initial conception to final analysis. Particular acknowledgements to Rosmin Ennis, Sarah Heidmann, Viktor Brandtneris, Alex Gutting, Kristen Ewen, Allie Durdall, and Kyle Jerris for their incredible work during the field stages of this work. This project was funded as an extension of the Territorial Coral Reef Monitoring Program, a collaborative program between the Center for Marine and Environmental Studies, The Coral Reef Initiative of the Coastal Zone Management Division of the Virgin Islands Department of Planning and Natural Resources, and the NOAA Coral Reef Conservation Program. This work was completed under Virgin Islands DPNR Fish and Wildlife Permit #18065U for Endangered Species Research and Export.

CONTRIBUTION OF AUTHORS

Dr. Tyler Smith acquired funding, assisted with experimental design and fieldwork, as well as guided the writing and editing process. Dr. Marilyn Brandt assisted with experimental design, statistical analysis, and editing. Dr. Sonaljit Mukherjee assisted with data acquisition and analysis of environmental data and editing. Dr. Monica Medina assisted with molecular design, molecular data analysis, and editing.

TABLE OF CONTENTS

	<u>Page</u>
Introduction.....	1
Mesophotic coral ecosystems.....	3
Corals in shallow reefs and MCEs.....	4
Methods.....	8
Site Selection.....	8
Lesion Generation.....	8
Physical Parameters.....	12
DNA Extraction and Amplification of Symbiodiniaceae.....	13
Statistical Analyses.....	16
Results.....	19
Physical Parameters of Sampling Locations.....	19
General Observations of Lesion Recovery.....	26
Lesion Recovery Rates in Corals.....	29
Absolute Lesion Recovery Rates.....	29
Relative Lesion Recovery Rates.....	38
Pigmentation Recovery Rates.....	40
Shallow and Mesophotic Characteristics of Recovery.....	46
Symbiont Classification.....	49
Discussion.....	55
Physical Properties of Locations.....	55
Physical Effects Modeling.....	56
Differences in Recovery between Shallow Water and Mesophotic Corals...	60
Conclusions.....	62
Bibliography.....	66

LIST OF FIGURES

<u>Figure</u>	<u>Page</u>
1. Map of the northern US Virgin Islands.....	9
2. Principal Component Analysis of physical parameters of each sampling location with depth.....	22
3. Principal Component Analysis of physical parameters of each sampling location without depth.....	24
4. Principal Component Analysis of physical parameters of each sampling location without depth separated by timepoint.....	27
5. Example of <i>A. lamarcki</i> lesion recovery.....	30
6. Example of <i>O. franksi</i> lesion recovery.....	30
7. Measured absolute lesion recovery rate of corals measured across depth with model prediction line.....	36
8. Measured absolute lesion recovery rate of corals measured across depth separated by timepoint with model prediction line.....	37
9. Measured relative lesion recovery rate of corals across depth with model prediction line.....	39
10. Measured pigmentation recovery rates of corals across depth with independent species model prediction lines.....	41
11. NMDS Ordination of lesion recovery metrics distributed by species and depth category.....	47
12. NMDS Ordination of lesion recovery metrics distributed by species and timepoint.....	48
13. Density distributions of shallow and mesophotic absolute lesion recovery rate, relative lesion recovery rate, and pigmentation recovery rate, distributed by species.....	50
14. Density distributions of shallow and mesophotic absolute lesion recovery rate distributed by species and timepoint.....	51
15. Density distributions of shallow and mesophotic relative lesion recovery rate distributed by species and timepoint.....	52
16. Density distributions of shallow and mesophotic pigmentation recovery rate distributed by species and timepoint.....	53

LIST OF TABLES

<u>Table</u>	<u>Page</u>
1. Location and site information for sampling locations.....	10
2. Measured physical parameters of shallow reef locations.....	14
3. Measured physical parameters of MCE locations.....	15
4. All possible response variables and terms for recovery rate mixed effects models.....	17
5. Pearson's r correlation coefficient values for physical parameters measured.....	20
6. P-values of of Pearson's r correlation coefficient values for physical parameters measured.....	21
7. Eigenvectors and Eigenvalues for principle component analysis (PCA) of physical parameters of each location with depth.....	23
8. Eigenvectors and Eigenvalues for principle component analysis (PCA) of physical parameters of each location without depth.....	25
9. Eigenvectors and Eigenvalues for principle component analysis (PCA) of physical parameters of each location separated by sampling period.....	28
10. Measured tissue recovery rates for each sampled colony separated by timepoint.....	31-32
11. Measured tissue recovery rates for each sampled colony over total sampling period.....	33-34
12. Significant multi-linear model outputs of recovery rates measured against depth and physical parameters.....	43-44
13. Significant mixed effects model outputs of recovery rates measured against depth and physical parameters through time.....	45
14. Summary of successful molecular genotyping of photosymbionts...	54

Introduction

Study of coral recovery is crucial in the continued understanding and conservation of coral reefs, some of the world's most biodiverse and productive ecosystems (Hoegh-Guldberg et al. 2007, Moberg & Folke 1999, Plaisance et al. 2011). As the foundational species of coral reefs, scleractinian corals must be able to recover from stress events. In many cases, acute stress events, such as hurricanes, disease outbreaks, runoff, and bleaching events can affect a given coral individual asymmetrically, and may cause death of tissue in only part of a coral colony (Fabricius 2005; Lugo-Fernández & Gravois, 2010). This is known as “partial mortality”, where the inflicted area, identified here as a “lesion”, can sometimes be regrown from the remaining living tissue on the colony (Loya 1976).

Tissue regrowth can be energetically expensive, and often requires re-allocation of energy away from other processes, such as growth and reproduction (Kramarsky-Winter & Loya, 2000; E. H. Meesters, Noordeloos, & Bak, 1994). Therefore, the rate of tissue regrowth can play a key role in overall reef resilience and recovery from major stress events. Stress and stress recovery is likely a key player in the overall location and structure of reefs in the large scale; Corals that prioritize stress recovery risk a competitive disadvantage when energy is taken from growth or reproduction for stress recovery (Anthony, Connolly, & Hoegh-Guldberg, 2007; Anthony et al., 2009; Maltby 1999); however, reef areas or specific corals with slower regrowth rates suffer increased risk of exposure to subsequent stress events while still recovering, resulting in additive damage to an already damaged reef ecosystem (Anthony, Connolly, & Hoegh-Guldberg,

2007; Levitan et al. 2014). An understanding of the factors that affect tissue regrowth rates, therefore, is directly tied to overall reef resilience.

Researchers have worked to identify key extrinsic and intrinsic factors that may affect tissue recovery. It is understood that lesion size, position, and even shape inherently alter lesion recovery rates, and lesion recovery rates have been shown to be specific to the species level (Hall, 1997; Loya 1976; Meesters et al., 1994; Meesters, Wesseling, & Bak, 1996; Oren, Benayahu, & Loya, 1997). Because of the energetic demand associated with lesion recovery, coral health also plays a key role (Fine, Oren, & Loya, 2002; Fisher et al., 2007; Ruiz-Diaz et al., 2016). Bleached coral colonies show slower rates of tissue regeneration compared to healthy counterparts in similar conditions (Mascarelli & Bunkley-Williams, 1999; Meesters & Bak, 1993a).

While coral survivorship is strongly tied with the external environment, sublethal physical gradients similarly affect coral processes, such as growth, health, and recovery. Coral tissue recovery rates have been closely tied to species-specific factors (Hall, 1997; Meesters, Bak, & Wesseling, 1996), as well as characteristics of the lesions themselves (Meesters, Bos & Gas, 1992; Meesters, Pauchli, & Bak, 1997; Oren & Loya 1997), however relating coral tissue recovery to the physical environment directly is less frequent (Nagelkerken, Meesters, & Bak 1999; Sabine et al., 2015). In many cases, tissue recovery can be delayed or even halted by stressful events during or immediately before recovery, such as thermal bleaching events, disease outbreaks, or sedimentation events (Henry & Hart, 2005; Meesters & Bak 1993; 1994). Beyond this, even day to day stresses of an environment, such as temperature fluctuations (Carilli, Donner, & Hartmann, 2012)

and wave energy (Dollar 1982), may prevent a given coral from recovering as fast as a competitor, or even a conspecific in a slightly different environment.

Mesophotic Coral Ecosystems

Deep-water or mesophotic coral ecosystems (MCEs), are coral ecosystems beyond 30m, or deeper than traditionally studied reefs. These systems have different environmental conditions than shallow reefs (Lesser et al., 2009), and are more vulnerable to different stress events compared to shallow water systems, such as destructive fishing practices and sedimentation (Smith et al. 2019a), and lower bleaching thresholds (Smith et al., 2016b). These differences in vulnerability are likely driven by the deeper water column, which alters the effects of major stress events such as storms and shallow water bleaching events, on the benthic ecosystem (Lugo-Fernández & Gravois, 2010; Smith et al., 2016a, Smith et al., 2016b). The differences in stress event experience may alter the probability of lesion formation following these stress events.

Causes and controls on stress events for MCEs likely differ from causes and controls on stress events for shallow water reefs, however daily environmental conditions such as temperature variation, water flow, and light level also change with depth. Tissue regeneration has largely been paired with surrounding water quality and coral health (Dikou & Van Woesik, 2006; Meesters & Bak, 1993; Sabine et al., 2015), and therefore distinct reef environments likely affect tissue recovery rates. Understanding reef resilience may be further confounded by different plastic responses by different species of corals at mesophotic depths, such as slowed growth rates (Brandtneris et al., 2016; Groves et al., 2018) and more fragile plating morphologies (Darling, et al., 2012). These

characteristics are highly specialized for dealing with overall lower-light conditions of deep reef environments, however the trade-off may be a decreased resilience following major stress events.

Although coral tissue regeneration and lesion recovery has been expansively studied for shallow water reefs, the effect of increased depth on tissue recovery has only recently been investigated (Counsell, Johnston, & Sale, 2019). Additionally, mesophotic coral stress response and recovery from stress has not been effectively studied (Smith et al. 2019a), despite a strong overlap of reef building species within shallow and upper mesophotic depths. In the US Virgin Islands, a majority of reef area is considered mesophotic (Smith et al., 2019b), much of which composes of coral that has survived multiple mass bleaching events, hurricanes, disease outbreaks, and many unknown stressors (Smith et al. 2019b). Some stress events may affect the shallow water environment more than the mesophotic, allowing nearby MCEs to possibly act as a refuge during these events. However stress events such as bleaching and disease outbreaks have been shown to also persist across depth, and possibly even occur only in MCEs. The ability of corals to recover from unavoidable acute stress is essential to the longevity of a reef system, regardless of depth.

Corals in shallow reefs and MCEs

In the US Virgin Islands, MCEs are largely built and structured by two genera: *Orbicella* spp. and *Agaricia* spp. (Smith et al. 2010). Each of these genera are commonly found in both shallow reefs and MCEs; however, both have adopted specific traits in deep water. *Orbicella franksi*, distinguished by exert wider spaced polyps and irregular

bumps across the surface, can be found in the US Virgin Islands as shallow as 3m depth and as deep as 45m. Across its depth range *O. franksi* has plastic “flattening” response in order to maximize light capture for photosynthetic carbon fixation by the coral’s endosymbiotic dinoflagellate of the family Symbiodiniaceae (Cairns, 1982; Dustan, 1975; Lajeunesse et al., 2018; Todd, 2008). However despite this morphological plasticity, MCEs dominated by *O. franksi* have been shown to have corals with reduced calcification and skeletal growth rates compared to conspecifics in shallow water (Groves et al. 2018; Weinstein et al. 2016). Additionally, individuals of *Orbicella faveolata*, a close relative to *O. franksi*, at mesophotic depth have been shown to have tissues with overall lowered energetic content compared to adjacent shallow reefs (Brandtneris et al., 2016). While this lowered metabolism allows *O. franksi* to persist in the upper mesophotic (30-45m), it may make this species slower to recover and more vulnerable to acute stress events and partial mortality.

Agaricia spp. is another key common reef building coral complex, with reef building species from 10m depth to 75m depth, much lower than *O. franksi*, however it also adopts a different strategy to persisting across different depth conditions. The abilities of *A. lamarcki* to act as a depth generalist has largely been attributed to pairing with depth-specialized symbionts in order to maintain similar growth rates across its entire vertical range (Bongaerts et al. 2013, 2015). Rather than changing morphology with depth, *A. lamarcki* builds expansive reef of flat, thin plates across shallow water and upper mesophotic (30-50m), only orienting more directly upward in the middle and lower mesophotic (Helmuth & Sebens, 1993; Smith et al., 2010). By partnering with depth-

specific symbionts and using a thin plating morphology, *A. lamarcki* can maintain growth and possibly maintain recovery rates across depth (Bongaerts et al., 2015). This would make *A. lamarcki*-dominated deep reefs more resilient to repeated stress events.

Along with considering lesion recovery response with depth, lesion recovery of both species likely responds to physical parameters independent of depth. While depth may be a key driver to changes in environmental conditions, particularly with transitions from shallow to mesophotic depths, comparison of tissue recovery against the environment directly will yield insight to some of the underlying processes that drive changes to lesion recovery with depth. As such, incorporation of these physical parameters directly into analysis will likely further explain trends in recovery rate, more than considering depth and species alone.

Additionally, while both are important habitat building corals in shallow and mesophotic depths, their inherently different characteristics across depth makes them separate and unique study species in the shallow and mesophotic. While stress recovery likely follows physical gradients, the distinct environments of shallow and mesophotic reefs likely will result in similarly distinct recovery profiles of both species. This has already been suggested with differences in morphology of *Montastrea cavernosa* (Studivan, 2019), as well as observations of morphology in *O. franksi* (Pandolfi & Budd, 2008) and depth-specific symbiont association in *A. lamarcki* (Bongaerts et al., 2013, 2015). This further supports the idea of MCEs as distinct and separate ecosystems from shallow water coral reefs.

Finally, the relationship between host corals and their photosynthetic endosymbiont is an important consideration in tissue recovery (Anthony et al., 2009). Because corals rely on the photosynthetic organisms to readily fix carbon to meet their needs, the abilities of the type of symbiont present may drive the corals' ability to harness energy for recovery (Iglesias-prieto & Schmidt, 2014; LaJeunesse et al., 2010). Association with different symbionts has been shown to have different trade-offs for the coral host, such as survival over heat stress events or maintaining calcification in low light environments (LaJeunesse et al., 2010). If different species of corals or even corals of the same species recover tissue faster, this may be attributed to association with specialized symbionts in this environment. While this has been shown previously as a possible mechanism for the wide depth range of *Agaricia lamarcki* growth (Bongaerts et al., 2015), it not been demonstrated in *Orbicella franksi*, which has a more limited depth range but can still survive and grow at mesophotic depths. Associating with depth-adapted symbionts or symbionts with highly plastic abilities is therefore a key driver in differences tissue recovery across depth.

With these combined approaches, the influence of external factors on lesion can be considered with respect to the observed relative differences across species and habitat. This is particularly important for MCEs, which currently have been identified as possible refugia from known reef stressors. As stress events such as storms and bleaching events continue to increase in frequency, understanding which areas or which corals may be more resilient following these events through faster recovery rates will be crucial for predicting the overall response of the entire reefscape.

Methods

Site Selection

This project aimed to study recovery of two major reef building species in shallow and deep reef environments across a range of physical environments. In order to decrease the likelihood of coastal influences, corals were sampled at 8 offshore sites previously identified by the Territorial Coral Reef Monitoring Program (TCRMP). Sites fell into two depth categories: shallow reefs (14-20m depth) and upper mesophotic (30-41m depth) (Figure 1). In addition to the previously established site at South Capella at 23m depth, a second, deeper reef (35m) was sampled to investigate possible site-specific effects not otherwise measured. All sites except the newly established deep site at South Capella have been monitored for coral health, diversity, and fish diversity annually since at least 2005. All data is publicly available at <https://sites.google.com/site/usvitcrmp> (See Table 1 for site and sampling day information).

Lesion Generation

Lesion generation methodology replicated coral laceration regeneration assay methodology originally developed by NOAA's Coral Disease & Health Consortium (NOAA, 2016). Moving out in a random direction from a haphazardly placed marker at each site, colonies of *O. franksi* and *A. lamarcki* ($n = 3$ for each species at each site) greater than 10cm in max diameter were identified and tagged using a cork tied to substrate using biodegradable twine. All colonies were upright, healthy, with no visible signs of bleaching or impaired health. After tagging and visual size estimation of the colony, a photo was taken of the colony surface facing downward using a Canon G1X

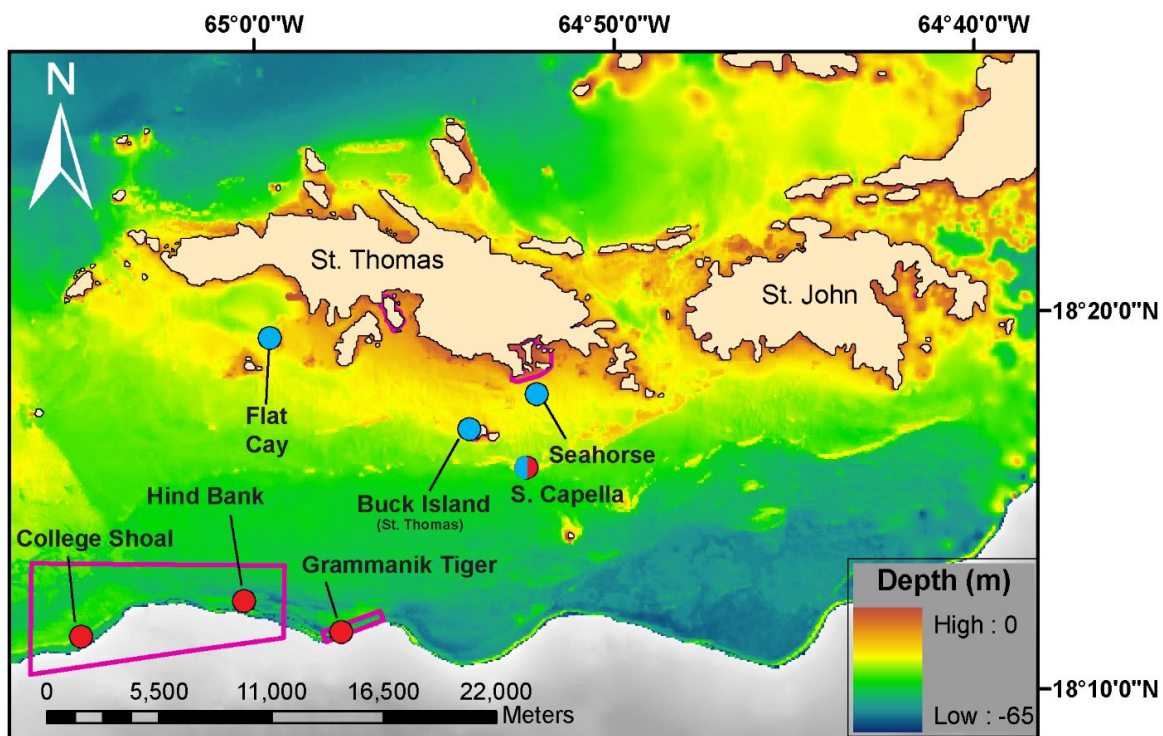


Figure 1) Map of St. Thomas and St. John with 8 sites previously identified by TCRMP, monitored annually since at least 2010. Surface color represents differences in depth of the sites and pink boundaries indicate marine reserves. Point color represents depth range (blue, red, and purple as shallow, mesophotic, and deep mesophotic, respectively). Original Figure adapted from <https://sites.google.com/site/usvitrmp/home>, accessed 02/18/2018

Table 1) Reef type, GPS coordinates, and depth of each lesion sampling site, previously identified by the Territorial Coral Reef Monitoring Program (TCRMP). MCE indicates “Mesophotic Coral Ecosystem”, beneath 30m. *indicates the newly established site. Lower Table indicates day each site was sampled for respective timepoints. Dates are listed here based on 5-digit Julian-Day.

Site	Reef Type	Latitude	Longitude	Depth (m)
Flat Cay	Shallow	18.31822	-64.99104	13
Buck Island	Shallow	18.27883	-64.89833	14
Seahorse Cottage Shoal	Shallow	18.29467	-64.86750	20
South Capella (Shallow)	Shallow	18.26267	-64.87237	23
South Capella (Deep)*	MCE	18.26267	-64.87237	35
College Shoal East	MCE	18.18568	-65.07677	30
Grammanik Tiger FSA	MCE	18.19113	-64.95032	38
Hind Bank East FSA	MCE	18.20217	-65.00158	41

Site	Initial Sampling	T1 Julian Day	T2 Julian Day	T3 Julian Day
Flat Cay	18134	18164	18194	18252
Buck Island	18134	18164	18194	18252
Seahorse Cottage Shoal	18134	18164	18194	18247
South Capella (Shallow)	18134	18164	18194	18247
South Capella (Deep)*	18134	18164	18194	18247
College Shoal East	18142	18172	18202	18251
Grammanik Tiger FSA	18142	18172	18202	18248
Hind Bank East FSA	18131	18161	18191	18248

camera. Using a small chisel or flathead screwdriver to mimic physical damage, a single circle of tissue approximately 2.5cm-diameter was removed from the colony and collected for later symbiont genotypic analysis. A second photo was then taken of the inflicted area following lesion generation. Colonies were then left on the reef to recover and revisited approximately every 30 days for 120 days following initial lesion generation (see exact dates of sampling in Table 1). Colonies were re-photographed with a standardized scale bar until the end of sampling, the coral colony marker was lost, or the coral appeared completely healed.

Lesion photos were imported and analyzed in Fiji, a modified version of ImageJ2, a Java-based open-source image processing program for analysis. In each photo the area of the lesion was calculated manually using the polygon selection tool and a scale bar placed in each photo. Change in that lesion area was then tracked over time with repeated sampling of the lesion in order to determine lesion recovery rates for each colony, called the ALRR. Lesion recovery was then also calculated based on the relative change in size of each lesion from start to finish of a given timepoint, called the RLRR.

At each timepoint, lesion recovery was measured three different ways: (1) the decrease in size of the lesion through time, or absolute recovery rate (ALRR), (2) the relative proportion of the original recovered tissue over time, or relative lesion recovery rate (RLRR), and (3) the change in color present in the lesion area through time or pigmentation recovery rate (PRR). These rates were then compared against depth for each species to determine the effect of increased depth on the rate of recovery from lesions.

For color recovery, images were converted to grayscale along a 0 to 255 color scale where healthy tissue was normalized to 0, or fully black in the image, and white coral skeleton in the image was scaled to 255, the maximum light value in an image. The lesion area from initial lesion generation was identified in each photo and the subsequent overall color value was measured within the lesion area. As a reference, an area of adjacent healthy tissue identical in size and shape to the lesion area was also measured for color value. The difference in these two values was then given as the relative difference in coloration between healthy tissue and lesioned tissue, and this difference was tracked through time as the pigmentation recovery rate (PRR).

Physical Parameters

In addition to depth, lesion recovery rates were mapped against temperature and benthic orbital velocity metrics from each location. All sites were monitored for physical parameters, including continuous monitoring of temperature using *in situ* subsurface temperature recorders (STRs) (HOBO Water Temp Pro v2, Onset Computer Corp., Bourne, MA). Probes have monitored temperature continuously at 15 minute intervals at sites since 2010, with all data publicly reported annually at <https://sites.google.com/site/usvitcrmp>. These data were gathered and analyzed during the exact period of study at each location. In order to accurately assess a more complete temperature profile, a daily temperature regime (daily average, daily maximum, daily minimum, and daily standard deviation) was calculated for each location starting and ending in the exact sampling window.

Benthic orbital velocity at each location was determined using a Simulated Waves Nearshore (SWAN) model reconfigured by the Caribbean Coastal Ocean Observation System (CariCOOS) for the US Virgin Islands, which calculated daily wave height, period, and wavelength experienced during the period that each site was sampled (Booij et al. 1999). For a full list of the precise study window of each location, see Table 1. Wave energy, subsequently, was translated to benthic orbital velocities (u) experienced by the corals at depth using linear wave theory (Smith et al. 2016), given as

$$1. \quad u = \frac{\frac{H}{2} g T_p}{\cosh\left(\frac{2\pi d}{L}\right)}$$

where d is the local water depth at the study site, H is the significant wave height, T_p is the peak wave period, and L is the local wavelength corresponding to the peak wave period and the local water depth. Similar to temperature, the wave energy environment was fully characterized using daily maximum, minimum, average, and standard deviations of calculated benthic orbital velocities for each location during the study period. For minimum benthic orbital velocity, the smallest calculated nonzero value was used for analysis. All calculated physical parameters can be found in Tables 2 and 3.

DNA extraction and amplification of Symbiodiniaceae

For each lesioned colony, all tissue removed as a result of the experimental lesion process was then collected and preserved in ethanol. From this tissue, the genetic relatedness of the symbionts present was analyzed using a PSB minicircle amplification technique. Zooxanthellae DNA was isolated using DNA Isolation Buffer in a

Table 2) Physical information about each shallow reef location that was sampled, organized by location, depth, and time period. Temperature metrics are measured in °C, benthic orbital velocity values measured in meters per second

Location	Sampling Period	Site Depth (m)	Average Temperature (°C)	Maximum Temperature (°C)	Minimum Temperature (°C)	Standard Deviation of Temperature (°C)	Average Benthic Orbital Velocity (m/s)	Maximum Benthic Orbital Velocity (m/s)	Minimum Benthic Orbital Velocity (m/s)	Standard Deviation of Benthic Orbital Velocity (m/s)
Flat Cay	T1	12.8016	27.68663039	28.27	26.9645	0.400058582	0.0031578	0.014098	0.000203	0.003184
	T2	12.8016	28.13547719	28.4065	27.85	0.123417894	0.0070479	0.049714	0.000179	0.011799
	T3	12.8016	28.68922021	29.215	28.0475	0.211706998	0.0013222	0.007101	1.95E-05	0.001427
	Total Period	12.8016	28.29434985	29.215	26.9645	0.489309069	0.0029104	0.049714	1.95E-05	0.005665
Buck Island	T1	14.0208	27.6708732	28.245	26.94	0.385683109	0.0511778	0.143367	0.014544	0.033627
	T2	14.0208	28.14289547	28.419	27.801	0.111228288	0.0639218	0.238075	0.015992	0.059131
	T3	14.0208	28.67016758	29.29	28.122	0.207967156	0.0339608	0.100481	0.002005	0.021764
	Total Period	14.0208	28.28267201	29.29	26.94	0.481929486	0.0446149	0.238075	0.002005	0.036206
Seahorse Cottage Shoal	T1	19.812	27.71289817	28.3075	27.124	0.389327948	0.008604	0.031075	0.001087	0.007103
	T2	19.812	28.17666128	28.394	27.875	0.109899596	0.0169836	0.091731	0.001031	0.022875
	T3	19.812	28.70735637	29.065	28.1345	0.188309867	0.0046275	0.016717	0.000123	0.004034
	Total Period	19.812	28.30241578	29.065	27.124	0.479164349	0.0082639	0.091731	0.000123	0.011804
South Capella (23m)	T1	23.1648	27.66166739	28.196	27.063	0.370611623	0.0609746	0.166824	0.017026	0.039344
	T2	23.1648	28.11283441	28.295	27.702	0.088602887	0.0732615	0.258883	0.020052	0.064148
	T3	23.1648	28.63740845	29.015	28.147	0.178322825	0.0441722	0.118045	0.00256	0.025645
	Total Period	23.1648	28.23896205	29.015	27.063	0.466013843	0.0551041	0.258883	0.00256	0.040778

Table 3) Physical information about each mesophotic location that was sampled, organized by location, depth, and time period. Temperature metrics are measured in °C, benthic orbital velocity values measured in meters per second

Location	Sampling Period	Site Depth (m)	Average Temperature (°C)	Maximum Temperature (°C)	Minimum Temperature (°C)	Standard Deviation of Temperature (°C)	Average Benthic Orbital Velocity (m/s)	Maximum Benthic Orbital Velocity (m/s)	Minimum Benthic Orbital Velocity (m/s)	Standard Deviation of Benthic Orbital Velocity (m/s)
College Shoal East	T1	29.2608	27.28235524	28.122	26.134	0.46925151	0.0618184	0.144289	0.020193	0.03573
	T2	29.2608	27.55641631	28.444	26.451	0.457733278	0.1155096	0.331626	0.034789	0.069986
	T3	29.2608	28.09343685	28.99	26.622	0.474601356	0.0549502	0.166201	0.003309	0.031705
	Total Period	29.2608	27.71907195	28.99	26.134	0.586430773	0.0695502	0.331626	0.003309	0.048361
South Capella (35m)	T1	35.3568	27.62479454	28.171	26.965	0.36814385	0.0609746	0.166824	0.017026	0.039344
	T2	35.3568	28.04621049	28.27	27.308	0.11787389	0.0732615	0.258883	0.020052	0.064148
	T3	35.3568	28.58817509	28.916	28.048	0.184709986	0.0441722	0.118045	0.00256	0.025645
	Total Period	35.3568	28.18677807	28.916	26.965	0.465842814	0.0551041	0.258883	0.00256	0.040778
Grammanik Bank	T1	38.4048	27.18305065	28.072	25.55	0.51412244	0.0655057	0.148171	0.021811	0.038817
	T2	38.4048	27.18159447	28.27	26.158	0.417687274	0.1260376	0.348449	0.03996	0.073204
	T3	38.4048	27.97579144	28.866	26.818	0.349318611	0.063445	0.178508	0.003844	0.035433
	Total Period	38.4048	27.51870556	28.866	25.55	0.578106897	0.0774341	0.348449	0.003844	0.052301
Hind Bank	T1	40.5384	27.01333585	28.097	25.671	0.568974821	0.080867	0.232025	0.019882	0.054888
	T2	40.5384	26.75302694	28.171	25.186	0.587899701	0.080383	0.192438	0.024197	0.051133
	T3	40.5384	27.65740458	28.766	26.207	0.441093677	0.064792	0.177074	0.003335	0.037135
	Total Period	40.5384	27.2580783	28.766	25.186	0.648132093	0.0747791	0.318335	0.003335	0.051372

microcentrifuge tube and resuspended with sodium dodecyl sulfate (SDS) and heated to 65°C for 30 to 60 minutes. Samples were then heated to 45°C in the presence of Proteinase K for 6 hours. If needed, the lysates were then chloroform-extracted once, phenol-extracted twice, and precipitated in ethanol at -20°C. Precipitates were be resuspended in 0.3 M sodium acetate, precipitated again with ethanol, and then resuspended in water and stored -20°C. The chloroplast minicircle plasmid from each Zooxanthellae was then amplified using a polymerase chain reaction (PCR) and when needed further cleaned using Exosap. The product was then submitted for sequencing, and analyzed using Molecular Evolutionary Genetic Analysis (MEGA). Successful sequences were then identified using the Blastn database and clustered using a minimum-distance hierarchical cluster analysis, determining relative relatedness of each sample from each species and depth category.

Statistical Analyses

All statistical analysis was completed using R statistical programming software version 3.5.2. In order to investigate variability of physical variables across location, a principal component analysis (PCA) using a correlation matrix determined the relative contributions of each physical variable to variability in the physical environment of each site, considering the maximum, minimum, average, and standard deviation of both temperature and benthic orbital velocity during the sampling time using the vegan package. Each lesion recovery metric was input with each of these metrics along with depth into multilinear and mixed effects models (all possible terms to be incorporated are listed in Table 3) using the lme4 package. These models were then tested iteratively

Table 4) Table of all possible mixed effects measured for mapping recovery rates of *Orbicella franksi* and *Agaricia lamarcki* across depth in both shallow and mesophotic environments. Each of the response variables was put into a separate mixed effects model, all mapped against the fixed effects and random effects. Each model was built as the most simple combination of fixed and random effects that maximized explanatory power without overfitting

Response variables (each separate models)	Possible Fixed Effects	Possible Random Effects
Relative Lesion Recovery Rate	Depth	Timepoint
Absolute Lesion Recovery Rate	Species	Location
Pigmentation Recovery Rate	Average temperature	
	Maximum temperature	
	Minimum temperature	
	Standard deviation of temperature	
	Average benthic orbital velocity	
	Maximum benthic orbital velocity	
	Minimum benthic orbital velocity	
	Standard deviation of benthic orbital velocity	
	Coral Colony Size	
	Initial lesion size	

ranging from the most simplistic model (simple linear regression of recovery against depth alone, referred to as the “null” model for each metric) to the most complex (including all random physical parameters within the same equation, referred to as the “saturated” model for each metric) in order to determine the most effective and simple model (referred to as the “ideal” or “fitted” model for each metric). Significance of terms within models was determined using Satterthwaite’s method, and significance of addition of terms through stepwise addition and deletion was determined using Wald’s chi-square method. All models were additionally tested for normality using by a shapiro test of the residuals.

Calculated lesion recovery metrics were combined with surface area to perimeter ratio in a non-metric multidimensional scaling (NMDS) ordination using a Euclidean dissimilarity matrix using the vegan package in R. Grouping of individuals was then compared using a permutational analysis of variance (PERMANOVA) the comparing centroids of dissimilarity of groups individuals of each species, depth category, and timepoint based on all four recovery metrics. Species and depth categories were then tested using a beta distribution analysis, a multivariate test of homoscedasticity. This allowed for an in-depth analysis of the variance and distributions of each of the recovery metrics grouped across species, depth category, and timepoint. Significant factors were subsequently tested iteratively for interactions of each factors.

Results

Physical Parameters of Sampling Locations

All measured and physical parameters input into the Principle Component Analysis are listed in Tables 2 and 3. An initial correlation analysis found that no variables significantly correlated with depth, and that standard deviation of temperature significantly correlated with average, maximum, minimum, and standard deviation of benthic orbital velocity (see Tables 5 and 6) and a shapiro-wilk multivariate normality test found the data to be normally distributed. The Principle Component Analysis of physical parameters measured found sites considered mesophotic were largely distinct from sites considered shallow (Figure 2). The exception was the shallow South Capella site, which was notably the deepest site of the sites considered shallow. The distinction between the two site types strongly followed along PC1 which had an explained 81% of total variance. On this axis average benthic orbital velocity was the primary contributor, followed closely by minimum benthic orbital velocity. There was additional spreading within both shallow and mesophotic groupings along PC2, which explained 13% of total variance. On PC2, standard deviation of temperature was the primary contributor (See Table 7). With PC1 and PC2 explaining 94% of total variance, these were the only axes fully assessed.

Because the sites were intentionally chosen with depth as the discriminating factor, the PCA was repeated with depth removed, to explore differences in the physical environment without bias. This PCA yielded a nearly identical distribution of points- on PC1, which again explained 81% of total variance (Table 8), average benthic orbital

Table 5) Pearson's r correlation coefficient values for physical parameters of each location

	Depth	Average Temperature	Maximum Temperature	Minimum Temperature	Standard Deviation of Temperature	Average Benthic Orbital Velocity	Maximum Benthic Orbital Velocity	Minimum Benthic Orbital Velocity	Standard Deviation of Benthic Orbital Velocity
Depth	1	-0.01	-0.96	-0.76	0.66	0.82	0.79	0.81	0.79
Average Temperature	-0.81	1	0.80	0.99	-0.97	-0.75	-0.71	-0.74	-0.71
Maximum Temperature	-0.96	0.80	1	0.73	-0.67	-0.73	-0.69	-0.69	-0.70
Minimum Temperature	-0.76	0.99	0.73	1	-0.97	-0.71	-0.67	-0.67	-0.67
Standard Deviation of Temperature	0.66	-0.97	-0.67	-0.97	1	0.61	0.57	0.59	0.56
Average Benthic Orbital Velocity	0.82	-0.75	-0.73	-0.71	0.61	1	0.99	1.0	1.0
Maximum Benthic Orbital Velocity	0.79	-0.71	-0.69	-0.67	0.57	0.99	1	0.99	1.0
Minimum Benthic Orbital Velocity	0.81	-0.74	-0.72	-0.70	0.59	1.0	0.99	1	0.99
Standard Deviation of Benthic Orbital Velocity	0.79	-0.71	-0.70	-0.67	0.56	1.0	1.0	0.99	1

Table 6) Respective p-values for Pearson's r-coefficient values of physical parameters of each location

	Depth	Average Temperature	Maximum Temperature	Minimum Temperature	Standard Deviation of Temperature	Average Benthic Orbital Velocity	Maximum Benthic Orbital Velocity	Minimum Benthic Orbital Velocity	Standard Deviation of Benthic Orbital Velocity
Depth	1	0	0	0	0	0	0	0	0
Average Temperature	0	1	0	0	0	0	0	0	0
Maximum Temperature	0	0	1	0	0	0	0	0	0
Minimum Temperature	0	0	0	1	0	0	0	0	0
Standard Deviation of Temperature	0	0	0	0	1	0.0001	0.0004	0.0002	0.0005
Average Benthic Orbital Velocity	0	0	0	0	0.0001	1	0	0	0
Maximum Benthic Orbital Velocity	0	0	0	0	0.0004	0	1	0	0
Minimum Benthic Orbital Velocity	0	0	0	0	0.0002	0	0	1	0
Standard Deviation of Benthic Orbital Velocity	0	0	0	0	0.0005	0	0	0	1

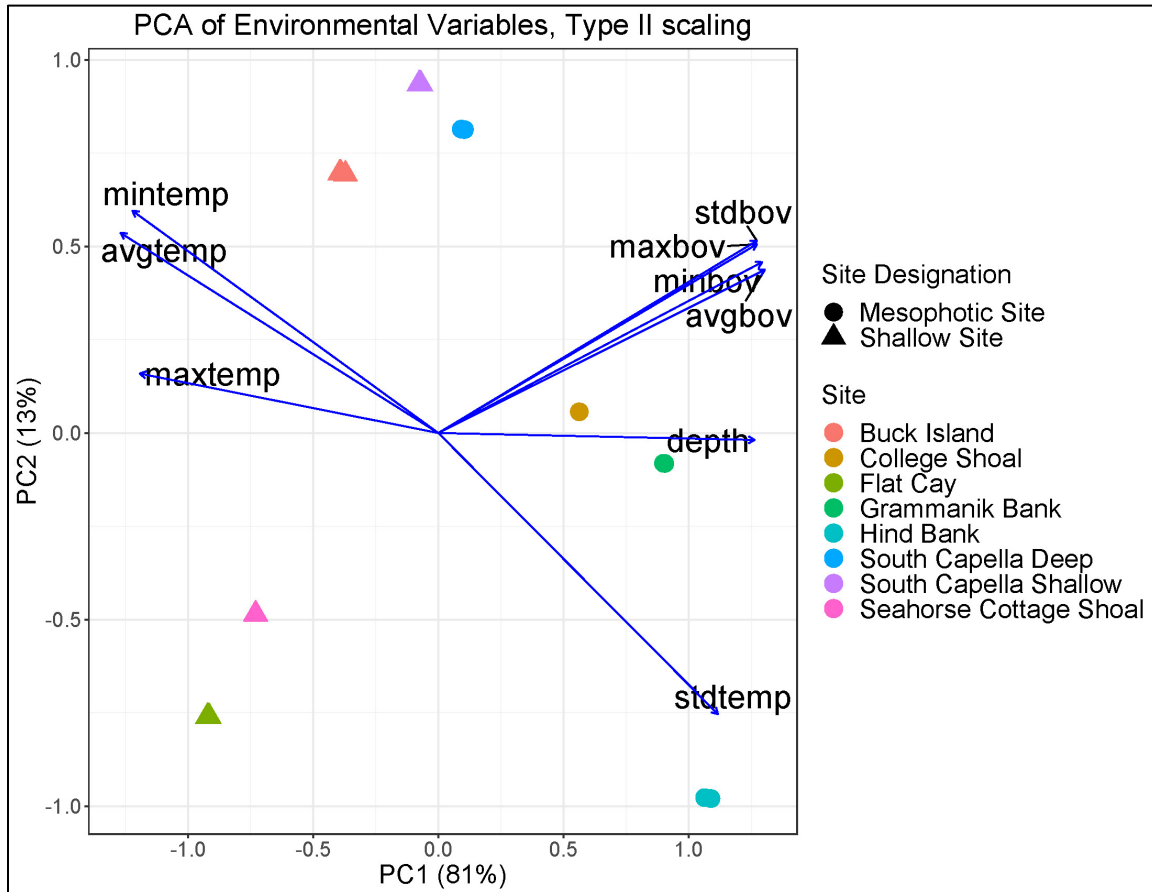


Figure 2) Principle Component Analysis (PCA) ordination of each site (color indicates site name, shape indicates depth designation, see adjacent legend), based on physical parameters measured throughout the sampling period. Arrows indicate direction of contributing axes, labeled appropriately. Note that “maximum”, “minimum”, and “standard deviation” are all abbreviated to “max”, “min”, and “std” respectively for clarity. Temperature and benthic orbital velocity are similarly abbreviated to “temp” and “bov” respectively.

Table 7) Summary of eigenvectors and eigenvalues for a principle component analysis (PCA) of physical data from each study location, with depth included.

	PC1	PC2	PC3	PC4	PC5	PC6	PC7
Eigenvalue	7.3160	1.1270	0.49830	0.036878	0.014035	0.004985	0.002782
Proportion Explained	0.8129	0.1252	0.05537	0.004098	0.002	0.0006	0.0003
Cumulative Proportion	0.8129	0.9381	0.99348	0.997577	0.999137	0.999969	0.999999

Species Scores	PC1	PC2
Depth	1.265	-0.019
Average Temperature	-1.270	0.536
Maximum Temperature	-1.194	0.159
Minimum Temperature	-1.223	0.596
Standard Deviation of Temperature	1.118	-0.75337
Average Benthic Orbital Velocity	1.306	0.438
Maximum Benthic Orbital Velocity	1.274	0.506
Minimum Benthic Orbital Velocity	1.295	0.458

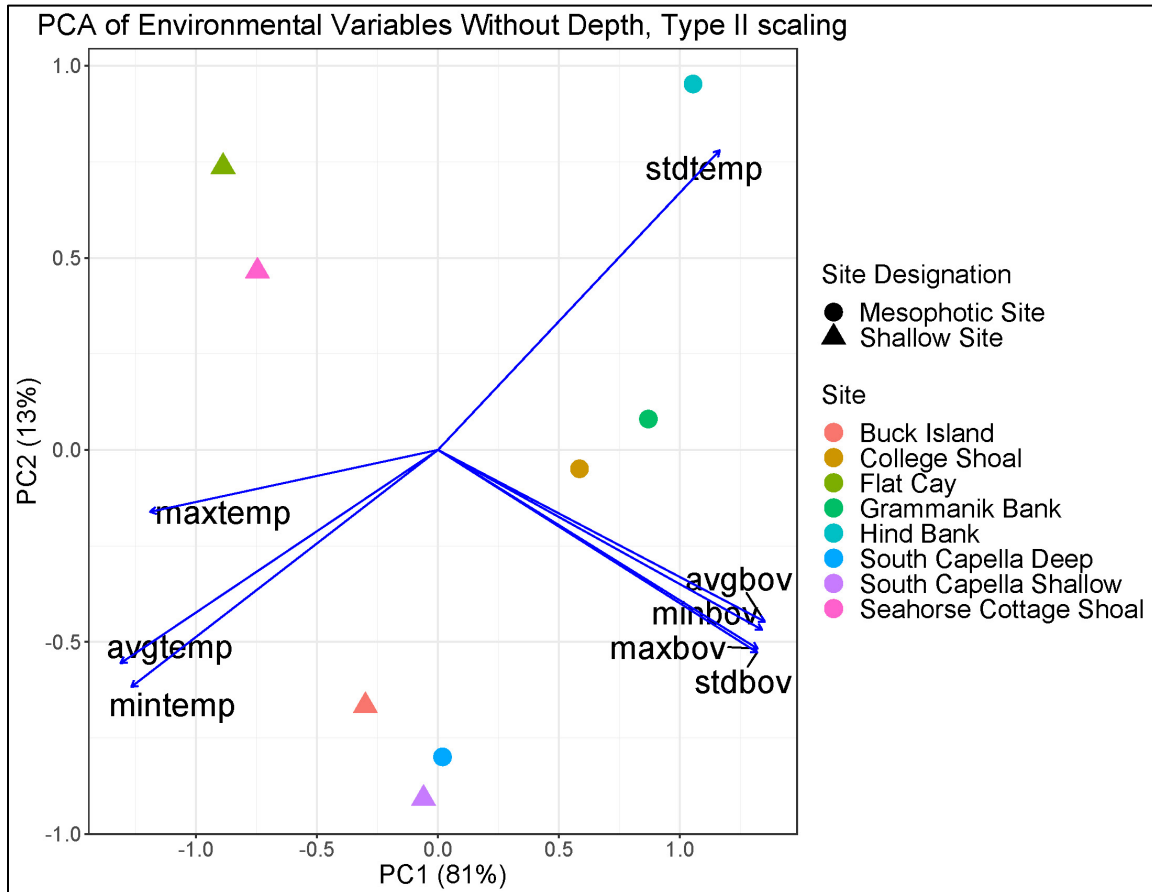


Figure 3) Principle Component Analysis (PCA) ordination of each site (color indicates site name, shape indicates depth designation, see adjacent legend), based on physical parameters measured throughout the sampling period with depth excluded. Arrows indicate direction of contributing axes, labeled appropriately. Note that “maximum”, “minimum”, and “standard deviation” are all abbreviated to “max”, “min”, and “std” respectively for clarity. Temperature and benthic orbital velocity are similarly abbreviated to “temp” and “bov” respectively.

Table 8) Summary of eigenvectors and eigenvalues for a principle component analysis (PCA) of physical data from each study location, with depth excluded.

	PC1	PC2	PC3	PC4	PC5	PC6	PC7
Eigenvalue	6.503	1.1268	0.33669	0.025055	0.0049857	0.0033736	0.00002
Proportion Explained	0.8129	0.1409	0.04209	0.003132	0.000623	0.0004217	0.00003
Cumulative Proportion	0.8129	0.9537	0.99582	0.998952	0.999575	0.99999	1.000

Species Scores	PC1	PC2
Average Temperature	-1.312	-0.5552
Maximum Temperature	-1.190	-0.1613
Minimum Temperature	-1.267	-0.6171
Standard Deviation of Temperature	1.165	0.7801
Average Benthic Orbital Velocity	1.351	-0.4473
Maximum Benthic Orbital Velocity	1.321	-0.5175
Minimum Benthic Orbital Velocity	1.340	-0.4684
Standard Deviation of Benthic Orbital Velocity	1.319	-0.5270

velocity and minimum benthic orbital velocity were still the primary contributing factors (Figure 3). PC2 similarly explained 15% of total variance (for a collective explanation 95% of total variance, all that was needed for analysis) and was the explanation for variation within depth category, and was driven by standard deviation of temperature and minimum temperature (see Table 8).

In order to assess if these physical distinctions were consistent through each sampling period of the study, the depth-excluded PCA was then repeated with the data broken into time periods. For all time periods, separation of mesophotic and shallow sites fell along PC1 (explained variance 65%; Table 9) with the primary factors being minimum benthic orbital velocity and average benthic orbital velocity (Figure 4). All timepoints similarly found overlap at the shallow South Capella location, which appeared similar to both shallow and mesophotic locations, however there was additional overlap of South Capella deep and Buck Island during T1. Shallow and Mesophotic sites again showed internal variability along PC2 (explained variance 25%) which again had standard deviation of temperature as the primary contributor. Table 9 contains a complete summary of the timepoint PCA along with respective Eigenvalues and Eigenvectors.

General Observations of Lesion Recovery

Lesion recovery was tracked over the complete 120-day period, a period longer than initially anticipated for lesions of this size. While some individuals did recover within the 60-day period, many individuals used the complete 120-day period for total recovery. Additionally, both species showed variability in recovery strategy that was not initially anticipated.

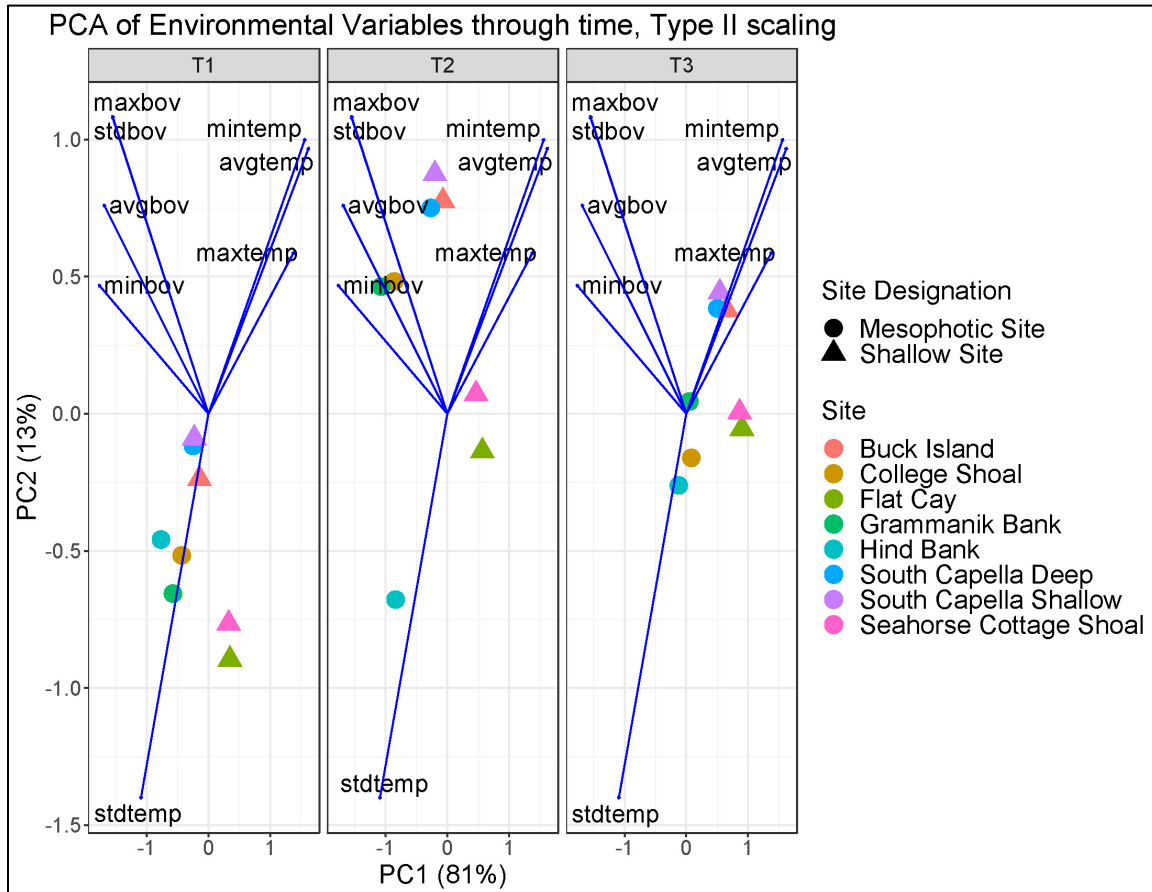


Figure 4) Principle Component Analysis (PCA) ordination of each site (color indicates site name, shape indicates depth designation, see adjacent legend), based on physical parameters measured during three specific timepoints during sampling. Arrows indicate direction of contributing axes, labeled appropriately. Note that “maximum”, “minimum”, and “standard deviation” are all abbreviated to “max”, “min”, and “std” respectively for clarity. Temperature and benthic orbital velocity are similarly abbreviated to “temp” and “bov” respectively.

Table 9) Summary of eigenvectors and eigenvalues for a principle component analysis (PCA) of physical data from each study location, with depth excluded and data split by sampling period.

	PC1	PC2	PC3	PC4	PC5	PC6	PC7
Eigenvalue	5.1661	2.0892	0.5720	0.09847	0.043899	0.014992	0.012391
Proportion Explained	0.6458	0.2611	0.0715	0.01231	0.005487	0.001874	0.001586
Cumulative Proportion	0.6458	0.9069	0.9784	0.99072	0.9962	0.998078	1.000

Species Scores	PC1	PC2
Average Temperature	1.601	0.9793
Maximum Temperature	1.366	0.5987
Minimum Temperature	1.540	1.0094
Standard Deviation of Temperature	-1.066	-1.4099
Average Benthic Orbital Velocity	-1.677	0.7601
Maximum Benthic Orbital Velocity	-1.532	1.0893
Minimum Benthic Orbital Velocity	-1.761	0.4742
Standard Deviation of Benthic Orbital Velocity	-1.530	1.0878

For *A. lamarcki*, many individuals showed fast recovery of deeper set tissues where polyp mouths are located, as these areas were less severely damaged during lesion generation. By later-phases of recovery, many individuals only needed to recover this top-level tissue (See Figure 5). For *O. franksi*, coral skeleton was re-colonized throughout the lesion before each polyp recovered completely, rather than from the border of the lesion. In this case, damaged polyps on the border of the lesion were sometimes first to fully recover (closing the lesion area), however, a number of individuals had isolated polyps regenerate from the center of the lesion at the same rate or faster than bordering polyps indicate tissue was not fully removed. This “infilling” regeneration from damaged polyps allowed some lesions to possibly recover faster in the same environment (see Figure 6).

Lesion Recovery Rates in Corals

Corals were monitored from initial marking until full health, or colonies were lost. For a full summary of lesion recovery values, see Tables 10 and 11.

Absolute Lesion Recovery Rates

When mapped against depth alone, linear regression of absolute recovery rate found no significant effect of depth for either species, nor a species and depth interactive effect. The null model overall showed significant but poor fit (adjusted $r^2 = 0.3023$, $p = 0.006079$). Continuing to include all environmental variables and colony factors to a saturated model improved model fit significantly ($r^2 = 0.8403$, $p < 0.0001$), however, Satterthwaite’s method found only initial lesion size had a significant effect on ALRR, showing small but significant positive correlation (slope estimate = 0.007901, confidence

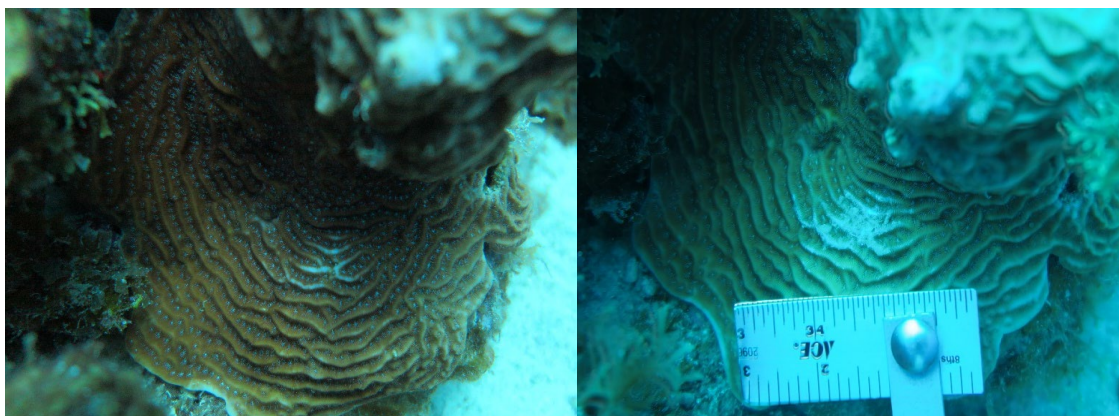


Figure 5) An example of an individual *A. lamarcki* that showed differential recovery between inset polyp areas and raised ridge areas that were damaged in lesion generation. The first photo (left) shows the lesion on the day of generation (T0) and the second photo (right) shows the same lesion 60 days later (T2). The lesion was fully recovered by the final timepoint.

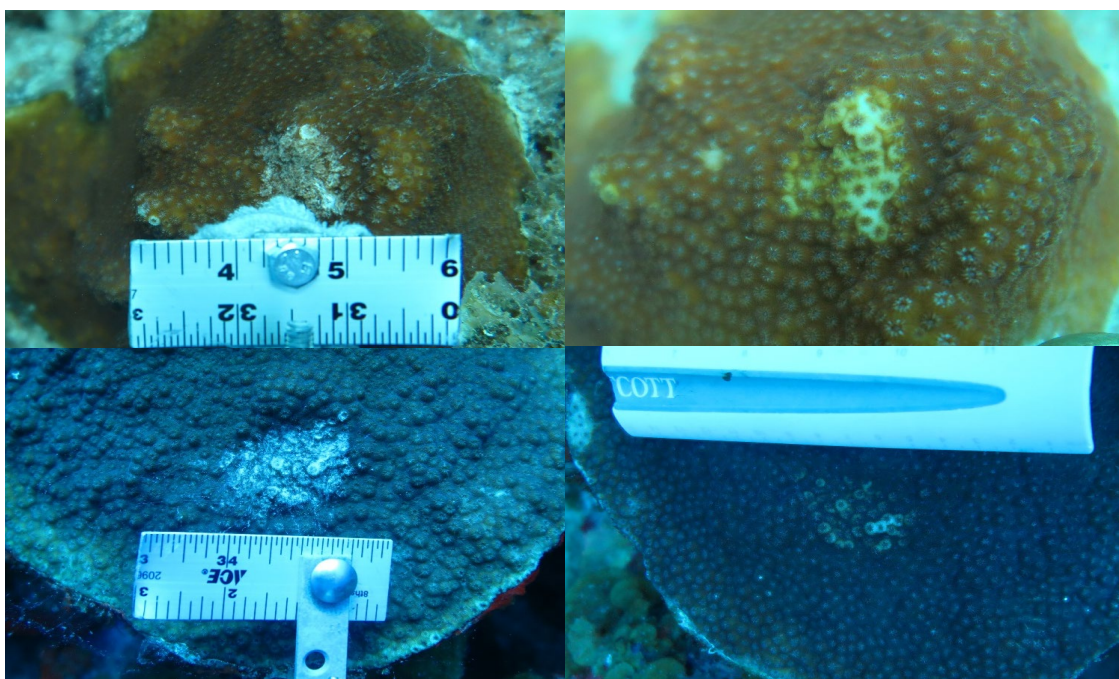


Figure 6) An example of the different methods of tissue regeneration by *O. franksi* during lesion recovery. Individuals first re-colonized the damaged skeleton completely, but following this colonization would either have polyps recover from the border of the lesion (top), or would have polyps recover from the middle of the lesion, expanding outward. Both left photos are from initial lesion generation, both following photos (right) are from 60 days later (T2).

Table 10) List of all recovery values (see text for details on abbreviations) for each sample period.

Location	Species	Colony	Depth	T1 ALRR	T1 RLRR	T1 PRR	T2 ALRR	T2 RLRR	T3 ALRR	T3 RLRR	T3 PRR
Flat Cay	<i>A. lamarcki</i>	AL-1	12.8	0.023226	0.005389	-0.01595	0.003440853	0.000952	0.002559	0.000444	-0.00166
	<i>A. lamarcki</i>	AL-2	12.8	0.012258	0.002969	-0.00111	NA	NA	NA	NA	NA
	<i>A. lamarcki</i>	AL-3	13.41	0.091828	0.033333	-0.00419	0	NA	-0.00473	NA	NA
	<i>O. franksi</i>	OF-1	12.8	-0.01484	-0.00397	-0.00868	0.015698893	NA	NA	NA	NA
	<i>O. franksi</i>	OF-2	13.11	0.008387	0.00197	5.93E-05	0.0129032	0.012024	-0.00821	-0.00313	0.003786
	<i>O. franksi</i>	OF-3	12.5	0.06215	0.015267	-0.02009	0.030537573	0.007115	-0.00479	0.011002	NA
Buck Island	<i>A. lamarcki</i>	AL-1	12.5	0.053978	0.019278	-0.00863	0.048602053	0.010929	-0.01039	NA	NA
	<i>A. lamarcki</i>	AL-2	14.33	0.086451	0.024632	-0.00332	0.035268747	0.033333	0.000701	NA	NA
	<i>A. lamarcki</i>	AL-3	14.63	0.096344	0.021242	-0.00676	0.010752667	0.029542	0.007268	0.017241	-0.0037
	<i>O. franksi</i>	OF-1	12.19	-0.00903	-0.00346	-0.01504	0.014623627	0.01223	-0.01177	-0.00871	-0.00313
	<i>O. franksi</i>	OF-2	12.5	0.055054	0.011642	-0.012	-0.006236547	0.003494	-0.00681	0.009327	-0.00424
	<i>O. franksi</i>	OF-3	11.89	0.002581	0.001042	NA	0.04064508	0.006093	NA	0.009471	NA
Seahorse Cottage Shoal	<i>A. lamarcki</i>	AL-1	19.81	0.033118	0.020952	-0.00403	0.048387	-0.01062	0.001233	-0.00739	0.000645
	<i>A. lamarcki</i>	AL-2	19.81	0.007312	0.00224	0.010988	0.00903224	0.013347	-0.00352	NA	-4.00E-05
	<i>A. lamarcki</i>	AL-3	19.51	0.031398	0.008675	0.003405	0.073118133	0.018072	-0.01377	0.005462	-0.00445
	<i>O. franksi</i>	OF-1	19.81	0.025591	0.008179	0.005052	-0.00387096	0.003825	-0.00388	0.005416	-0.00547
	<i>O. franksi</i>	OF-2	20.42	-0.00581	-0.00159	0.016144	-0.010537613	0.019112	-0.01376	NA	NA
	<i>O. franksi</i>	OF-3	19.81	0.059355	0.017326	-0.00042	0.016989213	-0.00235	0.000709	0.000207	-9.52E-05
South Capella (23m)	<i>A. lamarcki</i>	AL-1	22.86	0.038279	0.016667	-0.00174	-0.013763413	-0.00918	0.000115	0.010224	-0.00269
	<i>A. lamarcki</i>	AL-2	23.47	0.125161	0.029349	-0.00167	-0.01677416	0.033333	-0.00457	NA	0.003384
	<i>A. lamarcki</i>	AL-3	23.16	0.16043	0.028848	-0.0046	-0.00129032	-0.01839	0.002595	0.018868	0.001394
	<i>O. franksi</i>	OF-1	23.77	-0.02409	-0.01017	0.004755	0.03741928	-0.00543	-0.00524	0.002744	0.001003
	<i>O. franksi</i>	OF-2	22.56	-0.00301	-0.00097	-0.00688	0.015698893	-0.0004	0.012954	NA	NA
	<i>O. franksi</i>	OF-3	23.47	-0.01527	-0.00402	-0.00973	0.0129032	0.008788	-0.00404	0.001863	0.001554

Table 10 (continued from previous)

Location	Species	Colony	Depth	T1 ALRR	T1 RLRR	T1 PRR	T2 ALRR	T2 RLRR	T3 ALRR	T3 RLRR	T3 PRR
College Shoal East	<i>A. lamarcki</i>	AL-1	29.26	0.098494	0.02219	-0.00482	NA	NA	NA	NA	NA
	<i>A. lamarcki</i>	AL-2	29.26	0.188602	0.026918	-0.01969	NA	NA	NA	NA	NA
	<i>A. lamarcki</i>	AL-3	29.26	0.043011	0.007994	-0.01118	0.093118093	0.022766	0.002482	0.005077	-0.00536
	<i>O. franksi</i>	OF-2	29.26	0.074408	0.010353	-0.00217	NA	NA	NA	NA	NA
	<i>O. franksi</i>	OF-3	29.26	0.115914	0.015623	-0.00175	NA	NA	NA	NA	NA
South Capella (35m)	<i>A. lamarcki</i>	AL-1	34.14	0.029677	0.015541	-0.00659	0.006666653	0.00654	-0.00203	0.017234	-0.00753
	<i>A. lamarcki</i>	AL-2	36.27	0.028817	0.022222	0.005247	0.00516128	0.01194	0.002602	NA	NA
	<i>A. lamarcki</i>	AL-3	35.36	0.038495	0.013239	NA	0.019569853	0.012391	NA	0.018868	NA
	<i>O. franksi</i>	OF-1	34.14	0.019785	0.011705	0.013867	0.024946187	0.022745	-0.02048	NA	NA
	<i>O. franksi</i>	OF-2	35.05	-0.02903	-0.01793	0.003938	-0.009892453	-0.00397	0.018214	0.003057	0.007531
	<i>O. franksi</i>	OF-3	35.66	0.027097	0.018103	0.007918	-0.021505333	-0.03145	0.008928	-0.00394	-0.00478
Grammanik Bank	<i>A. lamarcki</i>	AL-1	38.71	0.139355	0.023736	-0.0132	0.01806448	0.010687	0.001096	0.021739	-0.00735
	<i>A. lamarcki</i>	AL-2	38.1	0.113763	0.01894	-0.00351	0.015268787	0.005887	-0.0036	0.017273	-0.00275
	<i>A. lamarcki</i>	AL-3	38.71	NA	NA	NA	NA	NA	NA	NA	NA
	<i>O. franksi</i>	OF-1	38.4	0.035269	0.0079	-0.00921	0.086236387	0.025316	-0.01349	0.021739	NA
	<i>O. franksi</i>	OF-2	38.4	0.12043	0.013391	-0.01756	0.026881667	0.004996	-0.00631	NA	NA
	<i>O. franksi</i>	OF-3	38.71	0.097204	0.020443	-0.00899	0.0612902	0.033333	-0.00708	NA	NA
Hind Bank	<i>A. lamarcki</i>	AL-1	40.54	0.069247	0.013621	-0.01152	NA	NA	NA	NA	NA
	<i>A. lamarcki</i>	AL-2	40.54	0.036344	0.012381	-0.01683	NA	NA	NA	NA	NA
	<i>A. lamarcki</i>	AL-3	40.54	-0.03226	-0.01761	0.009719	NA	NA	NA	NA	NA
	<i>O. franksi</i>	OF-1	37.49	-0.0471	-0.0154	-0.01648	0.118279333	0.026455	0.007418	-0.05962	-0.00391
	<i>O. franksi</i>	OF-2	37.49	-0.02108	-0.00918	0.002581	NA	NA	NA	NA	NA
	<i>O. franksi</i>	OF-3	40.54	0.048172	0.008953	-0.00946	NA	NA	NA	NA	NA

Table 11) List of all recovery values (see text for details on abbreviations) for the complete sampling period.

Location	Species	Colony	Depth	Total ALRR	Total RLRR	Total PRR
Flat Cay	<i>A. lamarcki</i>	AL-1	12.8	0.007545	0.001751	-0.00422
	<i>A. lamarcki</i>	AL-2	12.8	0.008639	0.002092	-0.00032
	<i>A. lamarcki</i>	AL-3	13.41	NA	0.008475	NA
	<i>O. franksi</i>	OF-1	12.8	0.001258	0.000337	-0.00347
	<i>O. franksi</i>	OF-2	13.11	0.010443	0.002452	-0.00021
	<i>O. franksi</i>	OF-3	12.5	NA	0.007167	NA
Buck Island	<i>A. lamarcki</i>	AL-1	12.5	NA	NA	NA
	<i>A. lamarcki</i>	AL-2	14.33	NA	NA	NA
	<i>A. lamarcki</i>	AL-3	14.63	0.038436	0.008475	-0.00169
	<i>O. franksi</i>	OF-1	12.19	-0.00115	-0.00044	-0.00835
	<i>O. franksi</i>	OF-2	12.5	0.02936	0.006209	-0.00687
	<i>O. franksi</i>	OF-3	11.89	0.013505	0.005451	NA
Seahorse Cottage Shoal	<i>A. lamarcki</i>	AL-1	19.81	0.004453	0.002817	-0.00044
	<i>A. lamarcki</i>	AL-2	19.81	NA	NA	0.001964
	<i>A. lamarcki</i>	AL-3	19.51	0.024322	0.00672	-0.00482
	<i>O. franksi</i>	OF-1	19.81	0.014502	0.004635	-0.00225
	<i>O. franksi</i>	OF-2	20.42	NA	NA	NA
	<i>O. franksi</i>	OF-3	19.81	0.014901	0.00435	3.15E-05
South Capella (23m)	<i>A. lamarcki</i>	AL-1	22.86	0.014388	0.006264	-0.00169
	<i>A. lamarcki</i>	AL-2	23.47	0.037739	0.00885	-6.97E-05
	<i>A. lamarcki</i>	AL-3	23.16	0.049215	0.00885	0.000121
	<i>O. franksi</i>	OF-1	23.77	-0.00622	-0.00263	0.000341
	<i>O. franksi</i>	OF-2	22.56	NA	NA	NA
	<i>O. franksi</i>	OF-3	23.47	0.008621	0.002269	-0.00293

Table 11 (continued from previous)

Location	Species	Colony	Depth	Total ALRR	Total RLRR	Total PRR
College Shoal East	<i>A. lamarcki</i>	AL-1	29.26	NA	NA	NA
	<i>A. lamarcki</i>	AL-2	29.26	0.048002	0.006851	-0.00239
	<i>A. lamarcki</i>	AL-3	29.26	0.040426	0.007513	-0.0048
	<i>O. franksi</i>	OF-2	29.26	NA	NA	NA
	<i>O. franksi</i>	OF-3	29.26	NA	NA	NA
South Capella (35m)	<i>A. lamarcki</i>	AL-1	34.14	0.016272	0.008521	-0.00582
	<i>A. lamarcki</i>	AL-2	36.27	NA	NA	NA
	<i>A. lamarcki</i>	AL-3	35.36	NA	0.00885	NA
	<i>O. franksi</i>	OF-1	34.14	NA	NA	NA
	<i>O. franksi</i>	OF-2	35.05	-0.00634	-0.00391	0.009413
	<i>O. franksi</i>	OF-3	35.66	-0.00097	-0.00065	0.002231
Grammanik Bank	<i>A. lamarcki</i>	AL-1	38.71	0.055386	0.009434	-0.00662
	<i>A. lamarcki</i>	AL-2	38.1	0.052526	0.008745	-0.0032
	<i>A. lamarcki</i>	AL-3	38.71	0.040292	0.00844	-0.00521
	<i>O. franksi</i>	OF-1	38.4	0.042118	0.009434	NA
	<i>O. franksi</i>	OF-2	38.4	NA	NA	NA
	<i>O. franksi</i>	OF-3	38.71	NA	0.009434	NA
Hind Bank	<i>A. lamarcki</i>	AL-1	40.54	0.01737	0.003417	-0.00594
	<i>A. lamarcki</i>	AL-2	40.54	NA	NA	NA
	<i>A. lamarcki</i>	AL-3	40.54	0.012462	0.006801	-0.00523
	<i>O. franksi</i>	OF-1	37.49	-0.00855	-0.00279	-0.00423
	<i>O. franksi</i>	OF-2	37.49	-0.00248	-0.00108	-0.00288
	<i>O. franksi</i>	OF-3	40.54	NA	NA	NA

intervals = 0.004 and 0.01, $p = 0.00019$). Stepwise addition and removal of terms yielded the best fit equation to include depth, species, average benthic orbital velocity, average temperature, initial size, standard deviation of temperature, and maximum benthic orbital velocity. This formula had substantially better model fit compared to the null model ($r^2 = 0.859$, $p < 0.00001$), driven by significant terms of average benthic orbital velocity (estimated slope = -2.629, $p = 0.0006$, CI = -3.997 and -1.261), average temperature (estimated slope = -0.1043, $p = 0.0201$, CI = -0.1906 and -0.0180), initial lesion size (estimated slope = 0.008022, $p < 0.00001$, CI = 0.0056 and 0.0104), standard deviation of temperature (estimated slope = -0.5246, $p = 0.0106$, CI = -0.9134 and -0.1357), and maximum benthic orbital velocity (estimated slope = 0.6575, $p = 0.000376$, CI = 0.3341 and 0.9808). Outputs of each of the linear models are summarized in Table 12. Neither depth nor species were significant terms, nor was there any significant interaction of species and depth for the ideal model fit (see Figure 7).

The regression was repeated looking at each timepoint individually (considering both timepoint as a random effect), again testing a fully saturated model and reducing terms to find the best fit model by incorporating average and maximum benthic orbital velocity, along with standard deviation of benthic orbital velocity (note that initial size was intentionally excluded from these analyses since samples were not independent of one another). This fitted mixed effects model similarly showed a stronger fit than a null model with depth and species alone ($r^2 = 0.4244$) with no significant effect for depth or species; however, both average benthic orbital velocity and standard deviation of benthic orbital velocity had an overall positive significant effect on recovery (average benthic

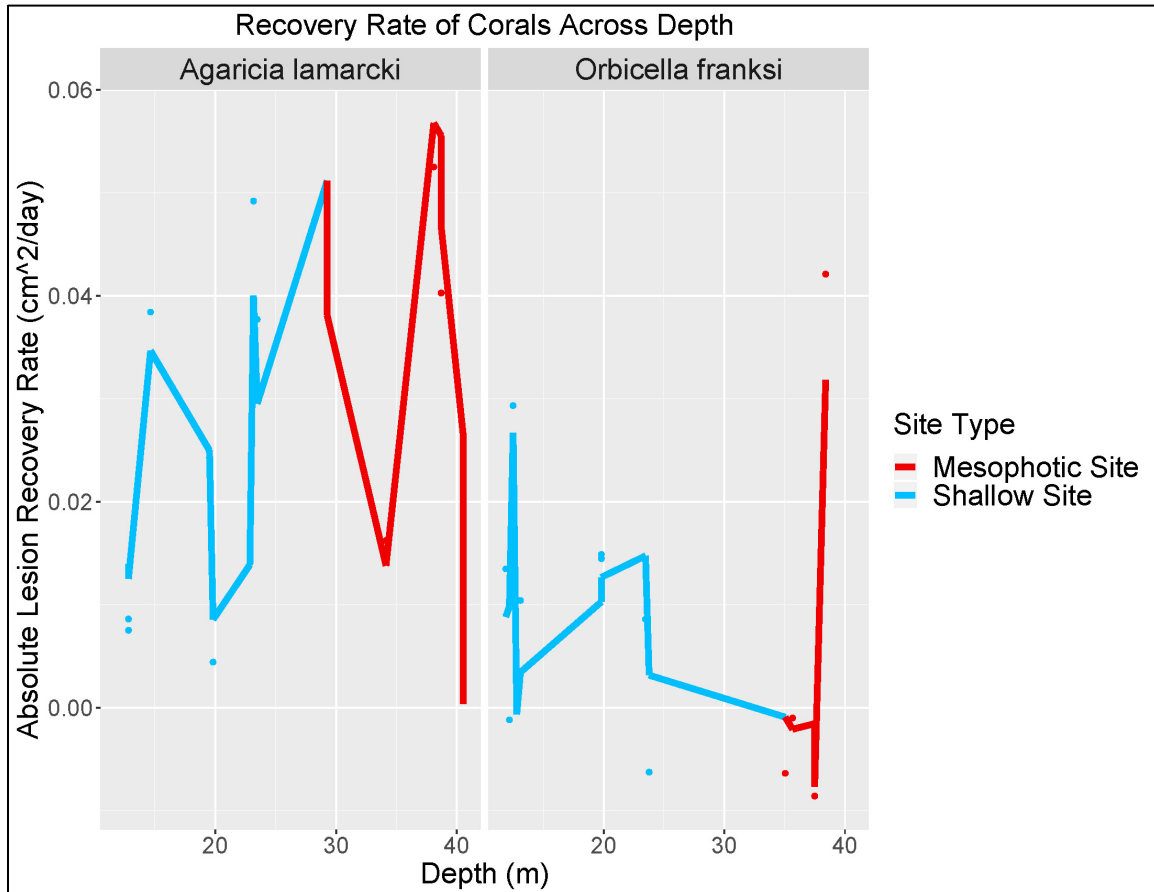


Figure 7) Measured absolute lesion recovery rate (cm²/day) measured across the depth (meters), separated by species (*Agaricia lamarcki* left, *Orbicella franksi* right). Colors represent depth designation individual or modeled area (blue and red representing shallow and mesophotic, respectively, see Figure legend). Points represent actual measured individuals, lines represent predictive outputs of the multilinear model.

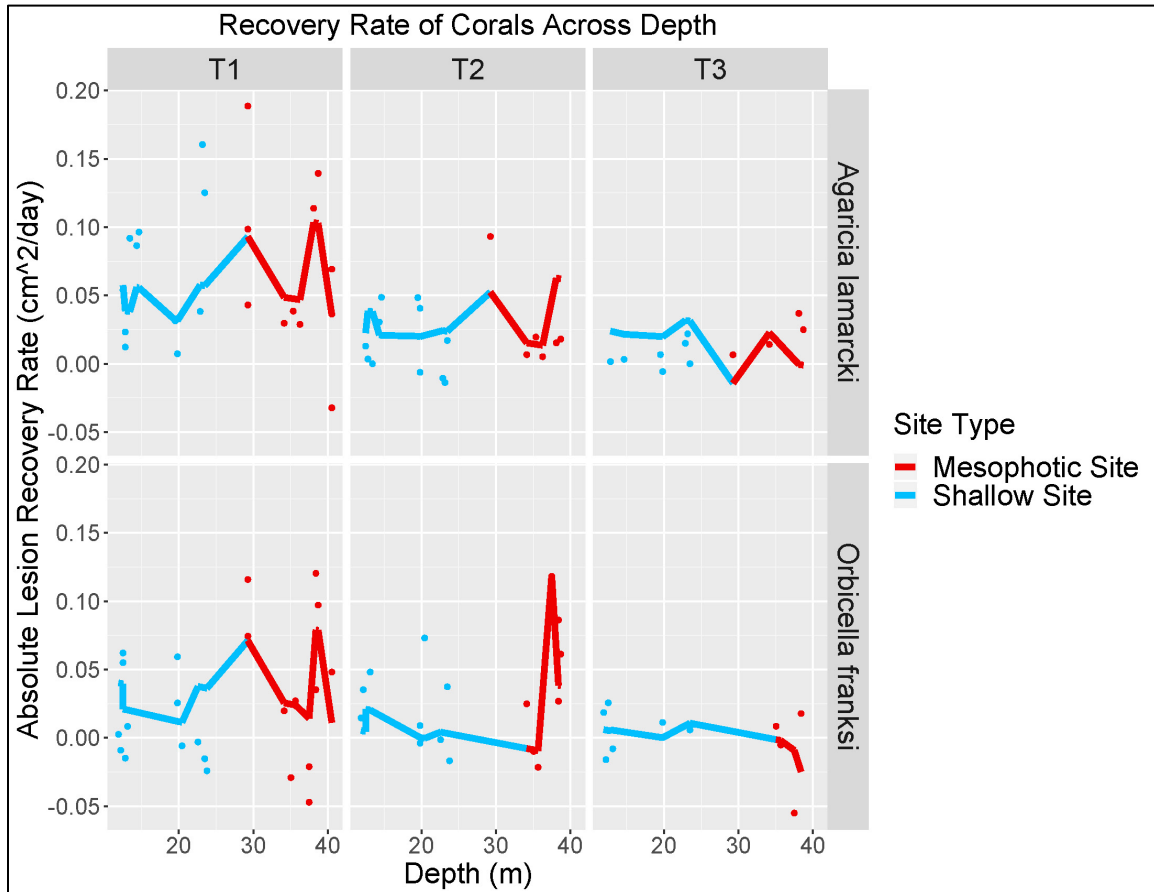


Figure 8) Measured absolute lesion recovery rate (cm²/day) during each timepoint, separated by species (*Agaricia lamarcki* on top, *Orbicella franksi* on bottom). Colors represent depth designation of each individual (blue and red representing shallow and mesophotic, respectively, see Figure legend). Points represent actual measured individuals, lines represent predictive outputs of respective mixed effects models.

orbital velocity had an estimated slope = 4.102, CI = 2.809 and 5.380, $p < 0.0001$; standard deviation of benthic orbital velocity had an estimated slope of 3.510, CI = 0.9716 and 6.0538, $p=0.00711$), and maximum benthic orbital velocity had an overall negative significant effect on absolute recovery (estimated slope = -2.207, CI = -3.041 and -1.374, $p < 0.0001$). Timepoint showed a significant effect on variance ($p = 0.01084$), indicating different results depending on stage of the recovery process (see Figure 8 and Table 13).

Relative Lesion Recovery Rates

When mapped against depth alone, regression of relative recovery rate (% of lesion recovered per day) found no significant effect of depth for either species, nor a species effect. The model overall showed significant but poor fit ($r^2 = 0.2618$, $p = 0.006867$). Incorporating all environmental variables and colony factors did not significantly improve model fit (adjusted $r^2 = 0.3733$, $p = 0.02494$, chi-square comparison of saturated model to null $p = 0.1814$), but found that both species and initial lesion size significantly affected variance in RLRR (p -values 0.00102 and 0.0193, respectively). Stepwise removal of nonsignificant terms yielded the best fit equation to include depth, species, and initial lesion size. This model again did not significantly improve model fit (adjusted $r^2 = 0.3524$, $p = 0.002043$, chi-square comparison against null model $p = 0.3894$). Within this model, initial lesion size positively affected RLRR (estimated slope = 0.0979, CI = 0.0100 and 0.1857, $p = 0.0302$), and both initial lesion size and species significantly affected variance in RLRR ($p = 0.00102$ and $p = 0.0193$, respectively, see Table 12 for full summary of model).

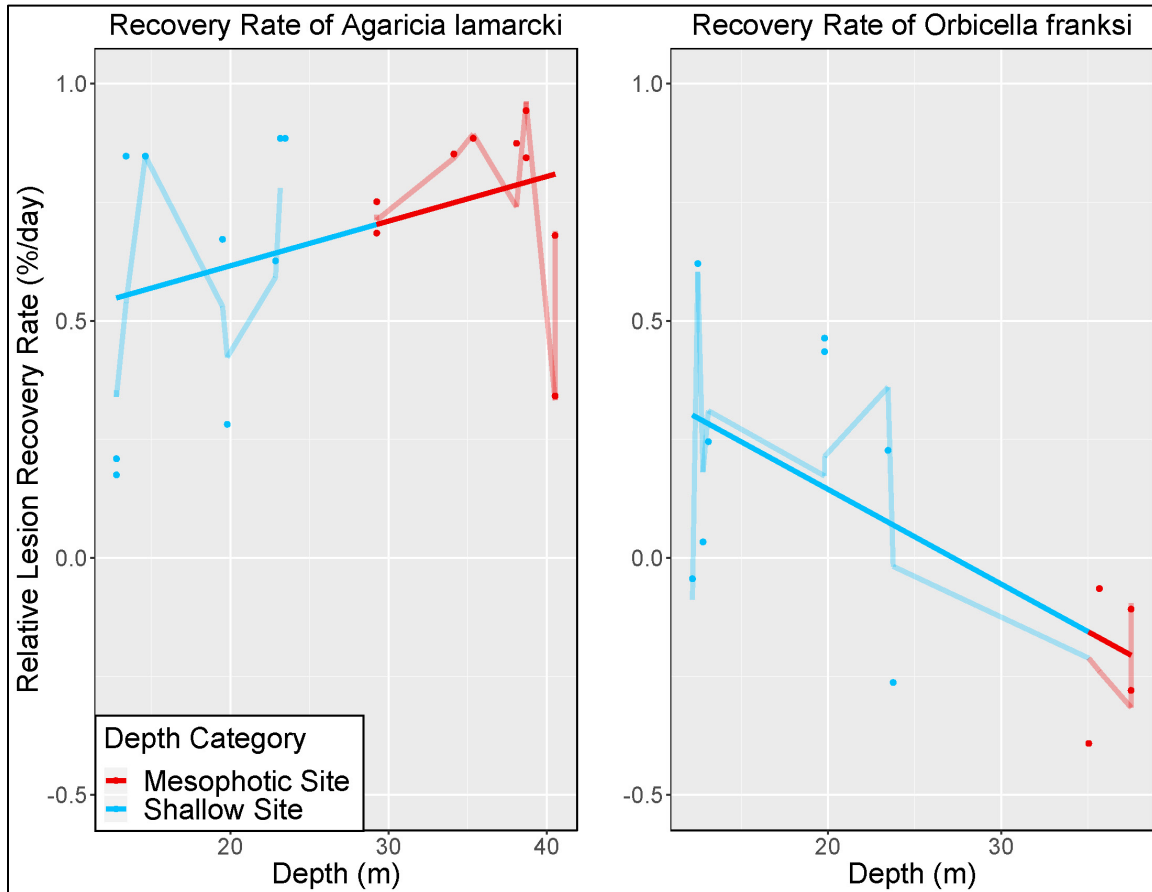


Figure 9) Measured relative lesion recovery rate (% of lesion/day) run independently for *A. lamarcki* (left) and *O. franksi* (right). Colors represent depth designation of points of model value (blue and red representing shallow and mesophotic, respectively, see Figure legend). Points represent actual measured individuals, lines represent predictive outputs of respective multilinear models, with standard linear models in bold and multilinear models faded for clarity.

Because species was identified as a significant contributor to the variance in combined RLRR models, two independent models for each species were developed (see Figure 9). Modeled against both depth alone and all measured variables, *A. lamarcki* had no significant relationships with any variables, with a non-significant model fit for each ($r^2 = 0.0901$, $p = 0.1208$; $r^2 = 0.4469$, $p = 0.1319$, respectively). For *O. franksi*, no addition of variables exceeded or improved the depth-only null model, which had a poor but significant fit ($r^2 = 0.3464$, $p = 0.0259$), and a significantly negative effect of depth (estimated slope = -0.02002, CI = -0.0371 and -0.0030, $p = 0.0259$, see Table 12).

Lack of successful sampling of *O. franksi* across all timepoints prevented adequate development of an effective combined mixed effects model or *O. franksi*-specific mixed effects model to incorporate timepoint or location into analysis. A separate model with just *A. lamarcki* was successfully developed, but found no significance of timepoint, location, depth, or any environmental or colony factors (see Table 13).

Pigmentation Recovery Rates

When mapped against depth and species alone, regression of relative pigmentation recovery rate (color value in lesion area recovered per day) showed overall significant but poor fit ($r^2 = 0.2461$, $p = 0.0238$). The null model found a significant effect of species (estimated slope = 0.0076, CI = 0.00098 and 0.0143, $p = 0.02618$) that also an interaction with depth (estimated slope = -0.00037, CI = -0.00061 and -0.0001, $p = 0.00467$) but no significant effect of depth overall. A significant positive species term indicated an overall tendency of *O. franksi* to have higher PRR in the dataset, with an

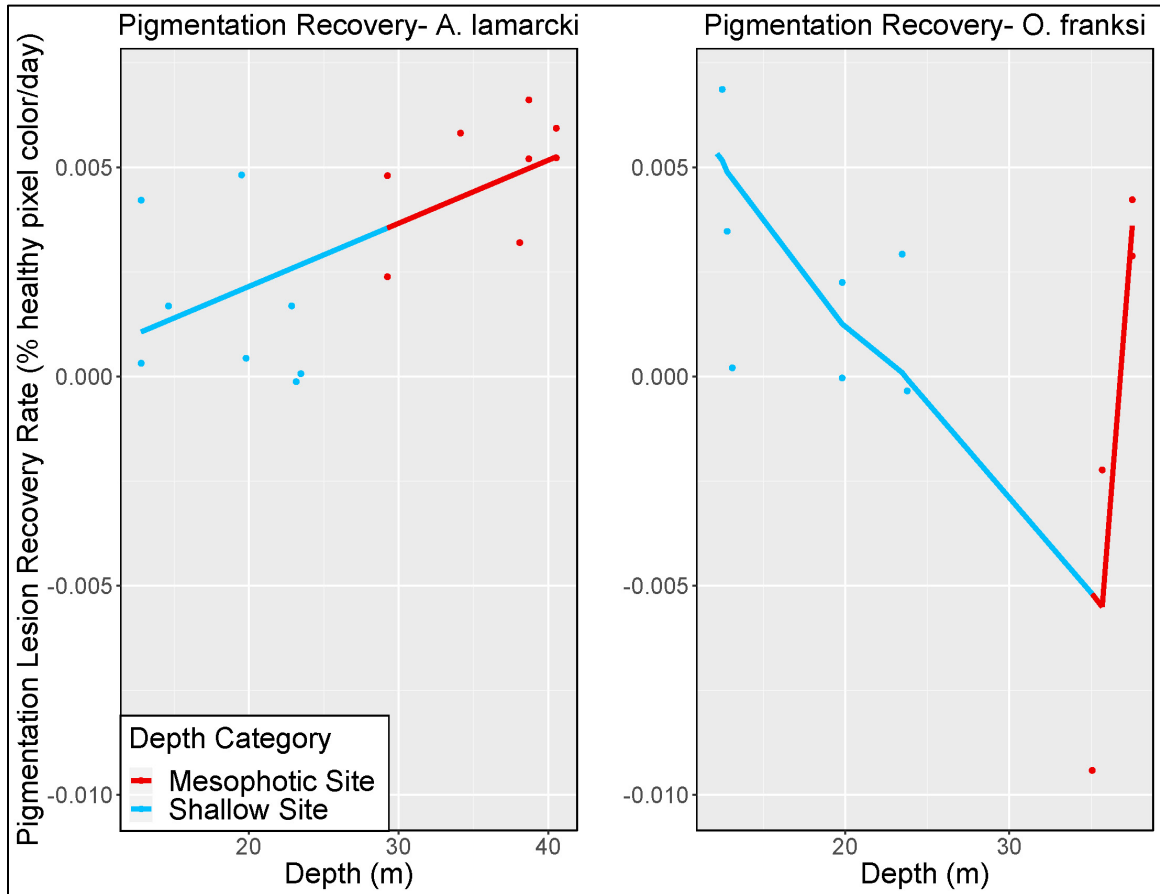


Figure 10) Measured pigmentation recovery rate of the lesion area (% color value/day compared to healthy tissue) run with both *A. lamarcki* (left) and *O. franksi* (right), combined. Colors represent depth designation of each individual or model output (blue and red representing shallow and mesophotic, respectively, see Figure legend). Points represent actual measured individuals, lines represent predictive outputs of respective mixed effects models.

interaction with depth. The model was then fully saturated with all environmental and colony factors had no significant terms and no significant improvement to model fit ($r^2 = 0.4512$, $p = 0.02925$, chi-square comparison against null model $p = 0.1137$). Stepwise removal of unnecessary terms left only average temperature in addition to depth and species (fitted model output in Figure 10). The resulting fitted equation had significantly improved model fit compared to the null model (adjusted $r^2 = 0.4693$, $p = 0.0008$, chi-square comparison against of fitted model to null model $p = 0.002903$). The fitted model found a similar effect as the null model for species (estimated slope = 0.0062, CI = 0.00053 and 0.0118, $p = 0.033$), along with a significant negative relationship with average temperature (estimated slope = -0.0072, CI = -0.0117 and -0.0027, $p = 0.0092$), and an opposing relationship with PRR and the depth-species interaction compared to the null model (estimated slope = -0.0003, CI = -0.0005 and -0.00009, $p = 0.00696$).

Because of the significance of both species and the interaction between species and depth in the fitted model, separate models were developed for each species (see outputs in Figure 10). For *A. lamarcki*, the null model of PRR mapped against depth alone had a poor but significant fit ($r^2 = 0.3825$, $p = 0.00632$), with a significant positive effect of depth on PRR (estimated slope = 0.00015, CI = 0.00005 and 0.00025). No additional environmental or colony variables improved model fit with any significance, including average temperature.

For *O. franksi*, the null model found no significant effect of depth. Stepwise removal and addition of environmental and colony variables found no significant terms to add to the null model except for average temperature. The species-specific fitted model

Table 12) Summary and significant outputs of linear models. For clarity, species-specific models were included only if they were significant. Absolute lesion recovery rate, relative lesion recovery rate, and pigmentation recovery rate are abbreviated to ALRR, RLRR, and PRR, respectively.

Recovery Metric	Model Type	r ² value	Model p-value	Significant Terms	Term p-value	Slope of terms	Lower 95% Confidence Bound	Upper 95% Confidence Bound
ALRR	Null	0.3023	0.006079	None				
	Saturated	0.8403	<0.0001	Initial Lesion Size	0.00019	0.007901	0.004	0.01
	Fitted	0.859	0.00001	Average Benthic Orbital Velocity	0.0006	-2.629	-3.997	-1.261
				Average Temperature	0.0201	-0.1043	-0.1906	-0.018
				Initial Lesion Size	<0.00001	0.008022	0.0056	0.0104
				Standard Deviation of Temperature	0.0106	-0.5246	-0.9134	-0.1357
				Maximum Benthic Orbital velocity	0.000376	0.6575	0.3341	0.9808
RLRR	Null	0.2618	0.006867	None				
	Saturated	0.3733	0.02494	Species (variance)	0.00102	n/a		
				Initial Lesion Size (variance)	0.0193	n/a		
	Fitted	0.3524	0.002043	Initial Lesion Size	0.0979	0.0302	0.01	0.1857
				Species (variance)	0.0193	n/a		
				Initial Lesion Size (variance)	0.00102	n/a		
	<i>A. lamarcki</i> Null	0.0901	0.1208	None				
	<i>A. lamarcki</i> Saturated	0.4469	0.1319	None				
<i>O. franksi</i> Null	0.3464	0.0259	Depth	0.0259	-2002	-0.0371	-0.003	

Table 12 (continued from previous)

Recovery Metric	Model Type	r ² value	Model p-value	Significant Terms	Term p-value	Slope of terms	Lower 95% Confidence Bound	Upper 95% Confidence Bound	
PRR	Null	0.2461	0.0238	Species	0.0076	0.02618	0.00098	0.0143	
				Depth*Species	0.00467	-0.00037	-0.00061	-0.0001	
	Saturated	0.4512	0.02925	Depth*Species	0.00799	-0.00036	0.00012	-3.057	
	Fitted	0.4693	0.0008	Species	0.033	0.0062	0.00053	0.0118	
				Average Temperature	0.0092	-0.0072	-0.0117	-0.0027	
				Depth*Species	0.007	-0.0003	-0.0005	-0.0001	
	<i>A. lamarcki</i> Null	0.3825	0.00632	Depth	0.00632	0.00015	0.0001	0.0003	
	<i>O. franksi</i> Null	0.1652	0.105	None					
	<i>O. franksi</i> Fitted	0.6064	0.0061	Depth	0.002	-0.00051	-0.0007	-0.0002	
				Average Temperature	0.0068	-0.0108	-0.0178	-0.0038	

Table 13). Summary and significant outputs of mixed effects models, with respective AIC and Loglik values. For clarity, only models with significant values and terms are included. Absolute lesion recovery rate and relative lesion recovery rate are abbreviated to ALRR and RLRR, respectively.

Recovery Metric	Model Type	AIC Value	LogLik	Significant Terms	p-value	Slope of terms	Lower 95% Confidence Bound	Upper 95% Confidence Bound
ALRR	Combined Fitted	-385.2	202	Average Benthic Orbital Velocity	<0.0001	4.102	2.809	5.38
				Standard Deviation of Benthic Orbital Velocity	0.00711	3.51	0.9716	6.0538
				Maximum Benthic Orbital Velocity	<0.0001	-2.207	-3.041	-1.974
				Timepoint (variance)	0.01084	n/a		
RLRR	<i>A. lamarcki</i> Fitted	374	-170	None				

found a significant negative effect of both depth (estimated slope = -0.00051, CI = -0.0007 and -0.0002, $p = 0.002$) and average temperature (estimated slope = -0.0108, CI = -0.0178 and -0.0038, $p = 0.0068$), with an overall significantly improved model fit (adjusted $r^2 = 0.6064$, $p = 0.006104$, chi-square comparison of fitted model to null model $p = 0.0068$). Lack of successful sampling of both species during timepoint T3 prevented adequate development of an effective combined or separate mixed effects model to incorporate timepoint or location into analysis.

Shallow and Mesophotic Characteristics of Recovery

NMDS analysis of relative lesion recovery rate, absolute lesion recovery rate, pigmentation recovery rate, and change to surface area to perimeter ratio during the complete sampling showed no clustering by either species or depth category (dimensions = 2, iterations = 20, stress = 0.001, see Figure 11). Separation of the analysis into individual species ordinations similarly yielded no major clustering or similarity (dimensions = 2, iterations = 20, stress = 0.001 for both). However, when ordination was split based on both timepoint and species, there is change in the spread of the data (dimensions = 2, iterations = 20, stress = 0.001).

For *A. lamarcki*, individuals in the shallow and mesophotic environment both began with widespread (diverse) responses in recovery, but grew to be increasingly similar to one another in subsequent timepoints, appearing quite tightly clustered by the final timepoint. Variance was retained longer with individuals from the shallow environment. For *O. franksi*, individuals in the shallow and mesophotic environment overall clustered together, but with different variance throughout the sampling

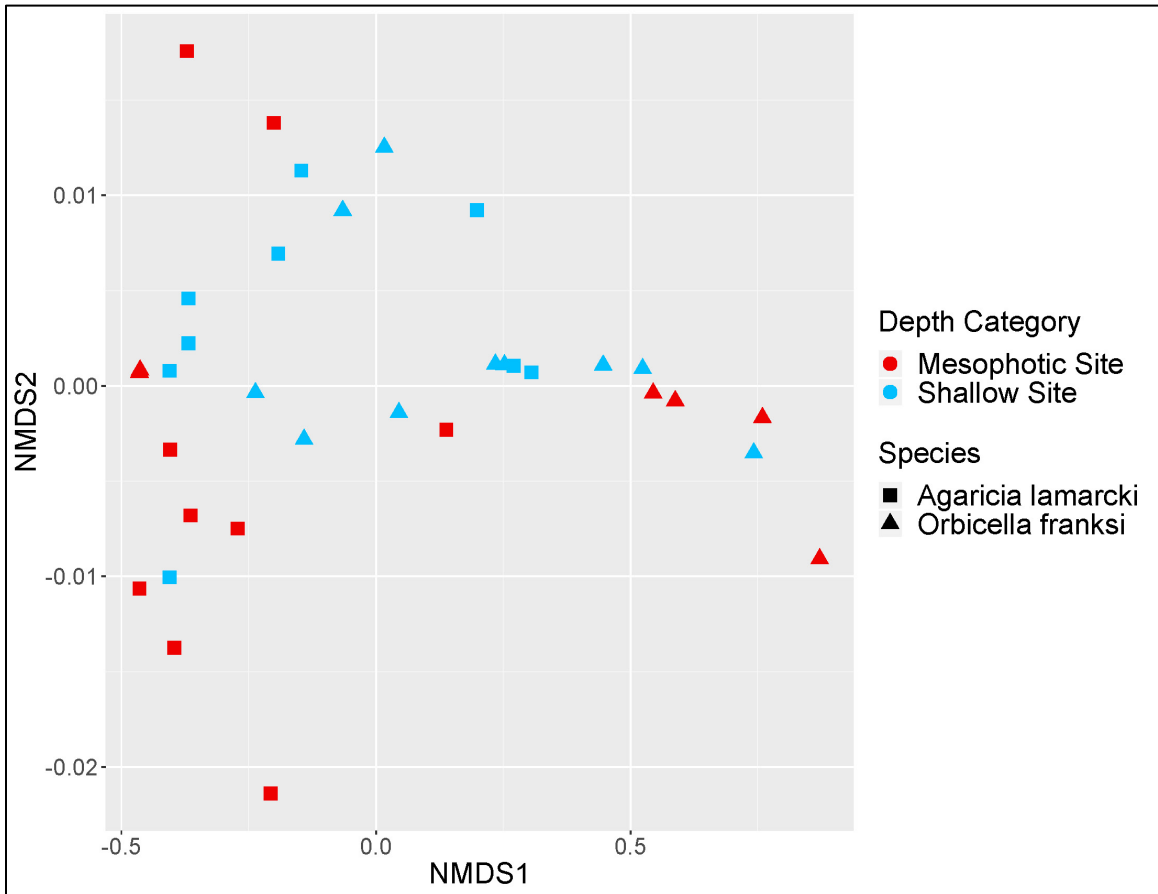


Figure 11) NMDS ordination of lesion recovery metrics using Euclidean dissimilarity, Color represents depth category of individual (red and blue for mesophotic and shallow, respectively) and shape represents the species of an individual (square and triangle for *A. lamarcki* and *O. franksi*, respectively).

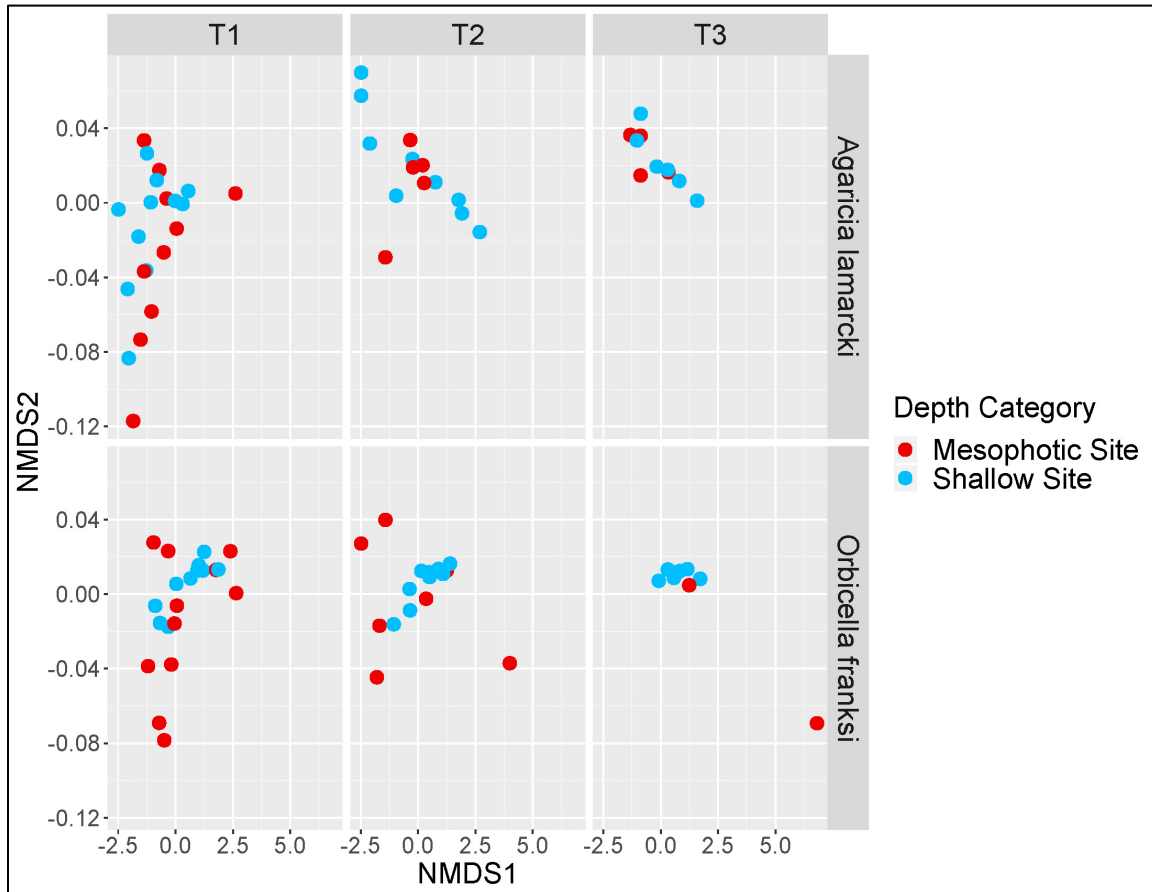


Figure 12) NMDS ordination of lesion recovery metrics using Euclidean dissimilarity, distributed by species and timepoint. Color represents depth category of individual (red and blue for mesophotic and shallow, respectively). Timepoints are labeled in order- T1, T2, and T3 represent the start, middle, and final stage of the experiment.

timepoints, with individuals in the mesophotic environment showing higher variability regardless of sampling time. The PERMANOVA comparing centroids of dissimilarity based on species, site type, and timepoint confirmed that species were significantly dissimilar to one another ($p = 0.001$), with no other significant factors or interactions.

Beta distribution analysis of the group dispersions amongst species, depth category, and timepoint yielded only one major factor- timepoint ($p = 0.001092$), indicating that the variance of each timepoint was overall different from each other without the overall variance changing based on species or depth category. When the data is split and tested separately for interactions of factors, group dispersion for *A. lamarcki* shows significant changes to variability based on both depth category and timepoint ($p = 0.02711$ and $p = 0.0008$, respectively, see Figures 13-16). Group dispersion for *O. franksi* shows significant differences in variability only across depth category and not timepoint ($p = 0.0002$ and $p = 0.1224$, respectively see Figures 13-16).

Symbiont Classification

Of the 48 individuals sampled, only 13 samples contained adequate genetic sample that could be successfully extracted and sequenced for symbiont identification (see Table 14). All 13 individuals were identified as *Cladocopium goreau*, historically identified as coral symbiont type C3. This species is considered one of the most commonly associated with stony corals worldwide (LaJeunesse et al., 2018).

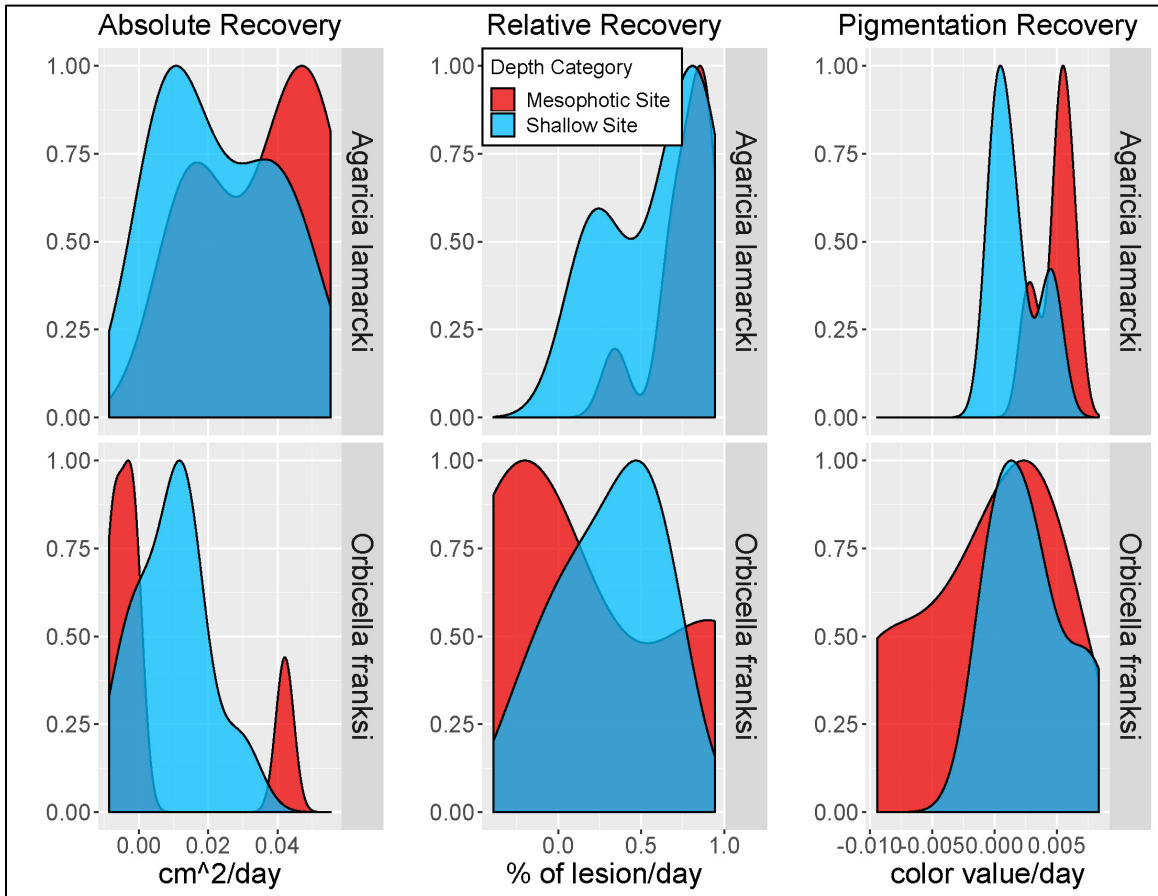


Figure 13) Density distributions of absolute recovery rate (cm²/day), relative recovery rate (% of lesion/day), and pigmentation recovery rate (% of healthy tissue coloration/day), split by species with *A. lamarcki* on top and *O. franksi* on bottom. Colors represent depth category of the distributions (red and blue for shallow and mesophotic, respectively).

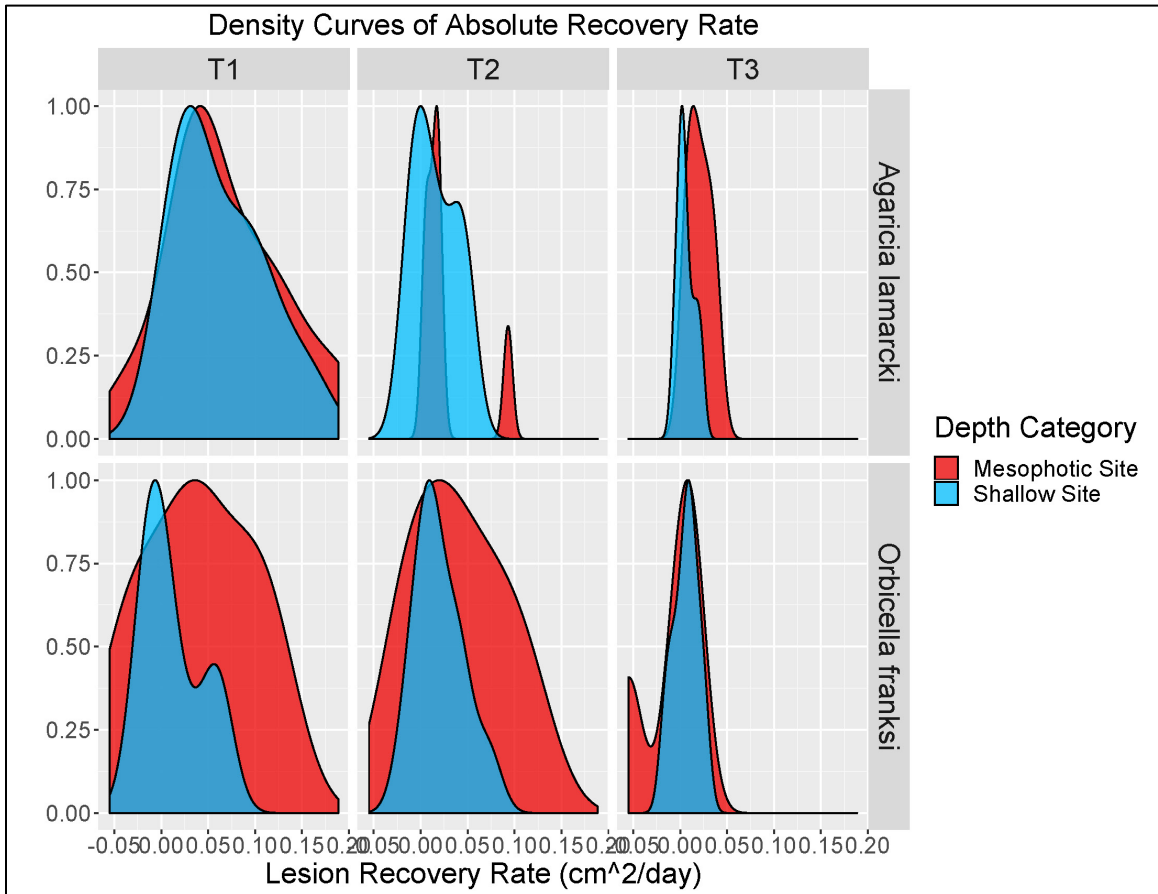


Figure 14) Density distribution of absolute recovery rate values (cm^2/day), split by both timepoint (beginning, middle, and end as timepoints T1, T2, and T3, respectively) and species (*Agaricia lamarcki* on top, *Orbicella franksi* on bottom). Colors indicate depth category of the distributions (blue and red for shallow and mesophotic, respectively).

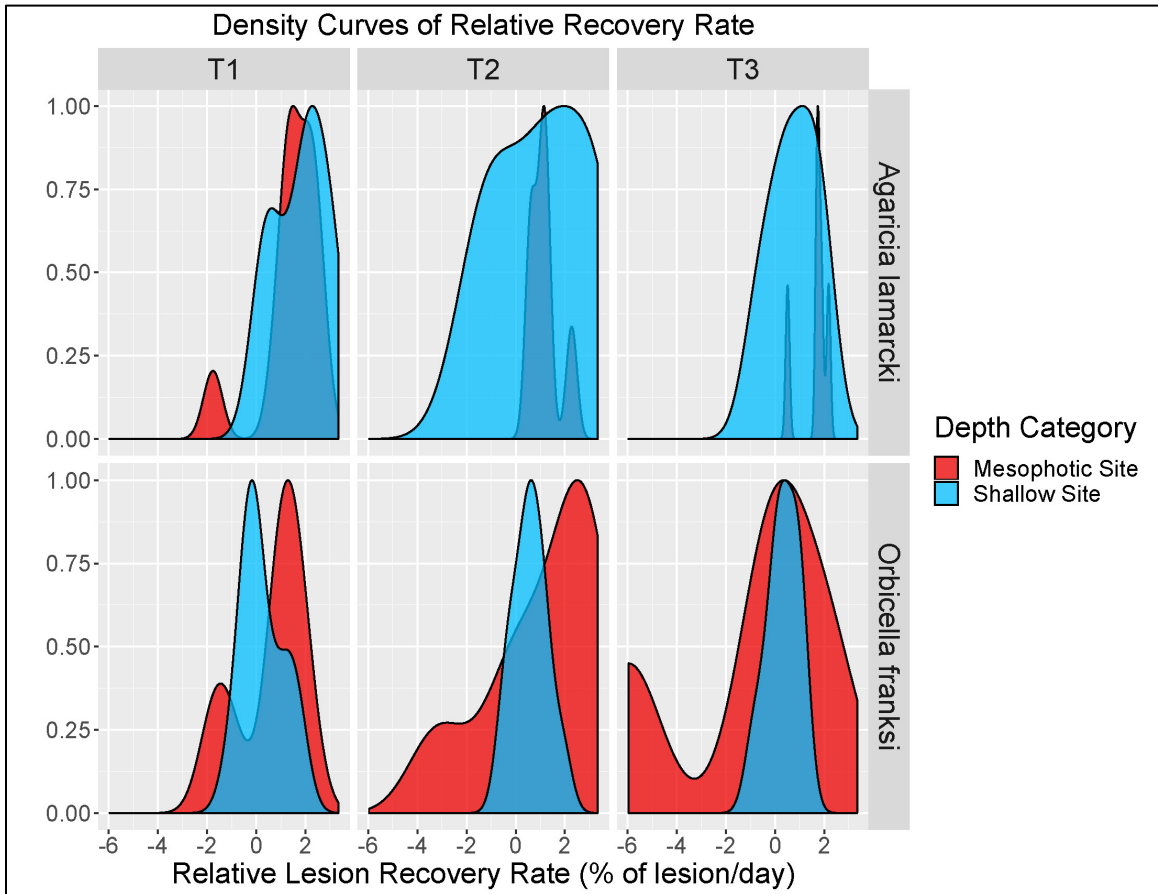


Figure 15) Density distribution of relative recovery rate values (% of lesion/day), split by both timepoint (beginning, middle, and end as timepoints T1, T2, and T3, respectively) and species (*Agaricia lamarcki* on top, *Orbicella franksi* on bottom). Colors indicate depth category of the distributions (blue and red for shallow and mesophotic, respectively).

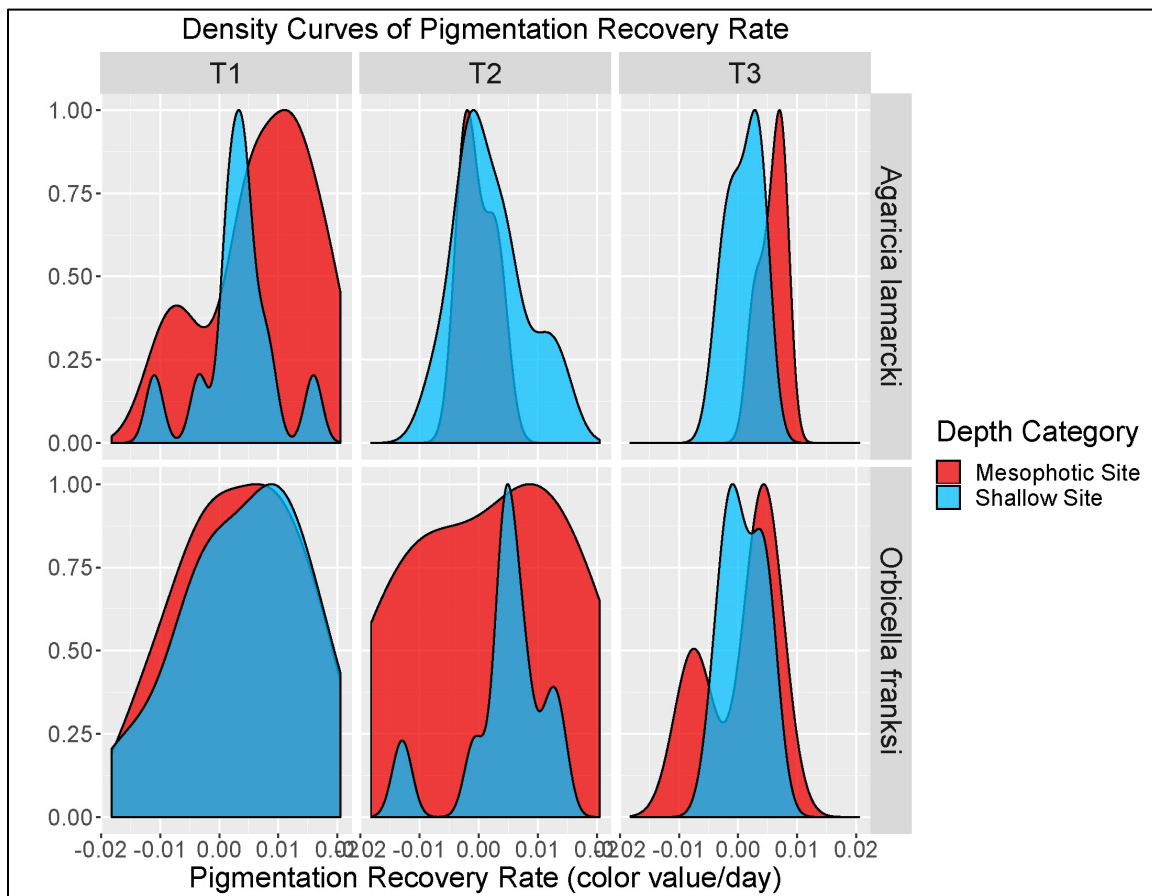


Figure 16) Density distribution of pigmentation recovery rate values (color value/day), split by both timepoint (beginning, middle, and end as timepoints T1, T2, and T3, respectively) and species (*Agaricia lamarcki* on top, *Orbicella franksi* on bottom). Colors indicate depth category of the distributions (blue and red for shallow and mesophotic, respectively).

Table 13) Identified symbionts with their respective coral host species, location and depth of sampling

Symbiont Species	Coral Host	Location	Depth
<i>C. goreau</i>	<i>O. franksi</i>	Flat Cay	13
<i>C. goreau</i>	<i>O. franksi</i>	Flat Cay	13
<i>C. goreau</i>	<i>O. franksi</i>	Flat Cay	13
<i>C. goreau</i>	<i>O. franksi</i>	Seahorse Cottage Shoal	20
<i>C. goreau</i>	<i>O. franksi</i>	South Capella (Shallow)	23
<i>C. goreau</i>	<i>O. franksi</i>	South Capella (Shallow)	23
<i>C. goreau</i>	<i>O. franksi</i>	South Capella (Deep)	35
<i>C. goreau</i>	<i>O. franksi</i>	Grammanik Tiger FSA	38
<i>C. goreau</i>	<i>O. franksi</i>	Hind Bank East FSA	41
<i>C. goreau</i>	<i>A. lamarcki</i>	South Capella (Shallow)	23
<i>C. goreau</i>	<i>A. lamarcki</i>	College Shoal East	30
<i>C. goreau</i>	<i>A. lamarcki</i>	South Capella (Deep)	35
<i>C. goreau</i>	<i>A. lamarcki</i>	Hind Bank East FSA	41

Discussion

Analysis of tissue recovery across depth for both a depth generalist (*A. lamarcki*) and a shallow-specialist at depth (*O. franksi*) showed distinct differences between two species within their complete overlapping depth range. Consistently *A. lamarcki* had no change to recovery with depth, with the exception of a significant increase in PRR as depth increased. When considered independent from *O. franksi* there were no instances where *A. lamarcki* recovery was significantly influenced by temperature or wave environment. While the depth range sampled represents the overlapping area at which both *O. franksi* and *A. lamarcki* occur with relative frequency, *A. lamarcki* persists and acts as a key reef builder in depths far beyond this study, documented in the US Virgin Islands over 70m deep (Smith et. al, 2015). Lack of significant relationships with any physical factors, colony variables, indicated that within this depth range, *A. lamarcki* acted relatively uniformly in terms of lesion recovery and tissue regeneration. This likely means that within its upper depth distribution lesion recovery is given equal priority regardless. By contrast, *O. franksi* recovery when considered separately from *A. lamarcki* was repeatedly negatively influenced by increased depth. Along with depth, *O. franksi* recovery was also affected by average temperature, demonstrating a possible thermal sensitivity within this range.

Physical Properties of Locations

While many of the physical parameters measured follow an overall depth-driven gradient, it is important to note that the relationship between these parameters and depth is not exact and that physical properties specific to each environment likely exert

influence on corals regardless of exact depth. Based on analysis of physical parameters of each site, the primary distinguishing factor between depth categories was benthic orbital velocity, with consistent distinctions between shallow and mesophotic environments stemming from various benthic orbital velocity metrics. Even more interestingly, physical differences alone are sufficient to create a significant differentiation between locations traditionally considered shallow and mesophotic, respectively. A significant distinction between shallow and mesophotic areas has been observed previously (Smith et al., 2019b), and though two sites that exist along the border of shallow and mesophotic exhibit physical properties of both environments, a site directly at the border (College Shoal East) had properties that were distinctly mesophotic. Temperature further exerted the most influence on variability and spread across within each depth category, indicating that within these depth designations variability in environment is largely temperature-driven.

Physical effects modeling

Considering both of these species together, ALRR showed was strongly influenced by benthic orbital velocity, more so than depth, species, or temperature. For absolute lesion recovery, all models consistently increased model fit with additional variables, but found no significant effect of depth for either species. The significant addition of timepoint, combined with all measured benthic orbital velocity metrics, indicates water movement may be the defining feature across locations that differentiates overall ability for tissue to reform and for lesions to close, regardless of species. Positive slopes of average benthic orbital velocity and standard deviation of benthic orbital

velocity indicates that higher water movements may assist recovery rates, however the negative slope of maximum benthic orbital velocity indicates that this relationship with benthic orbital velocity is limited; if the benthic orbital velocity experienced is overall too strong, or even experiences an anomaly of strong wave energy (such as a storm), recovery rates in the short term may suffer. This further supports the idea of influence of storm-based benthic orbital velocity on mesophotic community structure, which may be shaped by anomaly events over the long-term as well as short term recovery (Smith et al., 2016; Roberts et al. 2015).

RLRR models saw no change or improvements with the addition of environmental and colony variables, separation of the dataset to each species individually again showed distinction between *A. lamarcki* and *O. franksi*. While *A. lamarcki* RLRR showed no significant relationship with any environmental variables, colony variables, or timepoint, *O. franksi* RLRR had a significant negative relationship with depth. The negative slope of the model indicates that overall, as depth increases, *O. franksi* RLRR decreases, with no meaningful relationship with colony size, temperature, or benthic orbital velocity. This supports the hypothesis that while *O. franksi* and *A. lamarcki* are exist in high density at depth, *O. franksi* may be more limited at depth by lowered light or lowered metabolism (Brandtneris et al., 2016; Groves et al., 2018). *O. franksi* is only able to persist at depth by allowing trade-offs to growth, metabolism, and recovery (Brandtneris et al., 2016; Groves et al., 2018; Weinstein et al., 2016). The observed diversity in *O. franksi* recovery strategies (border recovery vs. infilling) and overall diversity of recovery in the mesophotic, confirmation by both RLRR and PRR that depth

negatively affects tissue recovery indicates that regardless of recovery strategy, tissue recovery is overall slowed as depth increases. Both metrics indicate that rates of recovery are lower as depth increases, revealing decreased recovery ability it approaches its lower depth limit.

A thermal sensitivity by *O. franksi* PRR recovery may be additionally supported by observations of lowered coral bleaching threshold in the mesophotic environment compared to shallow-water counterparts (Smith et al., 2016). With temperature as the defining feature explaining variation across the physical environment within each depth category, this may explain the wide spread of recovery rates of all metrics in the mesophotic-specific locations for *O. franksi*. While *A. lamarcki* may not show the same sensitivity to temperature, this is likely overshadowed by overall higher recovery in the mesophotic environment, indicating stronger adaptation to the deep-water environment.

When comparing the three recovery metrics, different elements of each of the developed models emerge, shedding some light on how these metrics measure recovery rate. ALRR, which is a standardized rate, was consistently affected by initial lesion size, indicating that the amount of tissue regenerated depended on the size of the area to be healed, as seen previously (Bak et al., 1977; Bak and Es, 1980; Meesters et al., 1996, 1997; Hall, 1997; Cróquer et al., 2002). RLRR, by looking at the proportion of recovery, inherently considers the size of the lesion during the healing process, and PRR measures recovery of healthy coloration regardless of lesion size, neither metric finding a meaningful contribution lesion size to best fit models of each. Aspects such as maximum lesion size (Bak and Es, 1980) and shape (Meesters et al., 1997) on coral tissue recovery is well

documented in literature, and while there was intention in this study was to constrain lesion size, even at this scale tissue recovery rates are modified in some respect. This effect is, however, the weakest effect in comparison to the effect of benthic orbital velocity, which had a stronger relationship with ALRR than initial lesion size, depth, or species. The significance of each of the metrics of benthic orbital velocity on ALRR likely indicates that wave energy likely determines the upper limit of tissue regeneration rates in both *A. lamarcki* and *O. franksi*. The importance of benthic orbital velocity, even at depth, has been documented as a key factor in reef structuring (Smith et al., 2016), meaning that likely corals, once settled, are acutely tuned into their wave environment.

For both species, the recovery process through time was significantly different for ALRR, but not for RLRR or PRR. This may be inherently true because as the lesions close and heal, there will be less change in actual area, although the change in coloration and relative size of the lesion may still move at a relatively constant rate. Similarly, variability decreases through each timepoint of the recovery process as the lesion tissue area grows smaller and more similar to one another. This further highlights the importance of considering lesion size when investigating recovery rates, and the non-significance of timepoint for both PRR and RLRR further corroborates the likely influence of lesion size on timepoint.

It is finally important to consider that while these models have significant relationships, large portions of the variance within the data remains unexplained, even with all available terms included. There are likely additional factors not considered here that significantly impact coral tissue recovery that were not possible in the scope of this

project. Within tissue recovery, tissue regeneration, and asexual polyp generation, there are a variety of factors associated with energy availability, such as heterotrophic opportunity and energy reserves, unidirectional water movement, that were not assessed here. Additionally, it is likely that many facets of location and individual that were not measured may exert some influence on lesion recovery. Differing recovery strategies and differences within coral individuals may be the result of genetic predisposition to specific physical environments, as well as some biological influences to recovery rates seasonally, such as preparation for spawning (Brandtneris et al., 2016). While all sites likely experience similar lack of coastal direct influence, the geographical spread of the sites sampled opens the possibility to differences in seasonal effects on temperature and wave energy. These seasonal affects may not have been detected during the sampling time (summertime in the USVI), but may affect settlement, phenotype, and morphology in the long term, potentially affecting the ability of an individual to recover tissue in the short term.

Differences in recovery between shallow water and mesophotic corals

Overall clustering of recovery showed no major differences aside from species, and in particular differences in clustering through time and depth may further suggest differences in depth specialization of each species. For *A. lamarcki*, while initial recovery is highly variable in both the shallow and the deep, variability only briefly occurred in the initial recovery period. Similarities in recovery of individuals likely suggests similar strategy or specialization for *A. lamarcki*, regardless of depth. Given the deeper range of *A. lamarcki*, shallow individuals sampled here likely exist within the upper to

intermediate depth distribution of the species, and therefore only in the shallowest locations may be an environment that slightly stressful in terms of possible excess light (Laverick and Rogers, 2018; Smith et al., 2015).

Regarding *Orbicella franksi*, individuals in the mesophotic environments were highly variable and, regardless of timepoint, did not cluster together. By contrast the individuals in the shallow water environment clustered tightly regardless of timepoint, indicating identical strategy and priority in the shallow water environment, but variability in the mesophotic. As opposed to *A. lamarcki*, this depth range represents the lower limits of *O. franksi*, which individuals may be found as shallow as 2m in the USVI (Smith et al., 2015). As such, individuals in the lower depth limit may be exhibiting varied responses to a more high-stress environment and likely light limitation in the mesophotic environment.

Interestingly, lack of diversity of symbionts suggests that differences in recovery abilities are host-driven, rather than specialized symbionts in the shallow or deep environment. This is a strong assumption, as the majority of the individuals in this study could not be analyzed or identified. In the future, this may be tested by investigating symbiont communities both within and beyond the range of overlap between the two species.

Conclusions

Analysis of some recovery metrics demonstrated a clear effect of depth on both species, with *O. franksi* tissue recovery primarily negatively affected by depth while *A. lamarcki* tissue recovery showed a neutral or positive association between recovery and depth. This indicates that there may increased success by *A. lamarcki* as a depth-generalist or even depth-specialist, while *O. franksi* may utilize trade-offs to persist at depth. Tissue regeneration rates in both species appears susceptible to benthic orbital velocity, a key factor in the physical environment on a reef and a primary distinguishing factor between shallow and mesophotic reef environments. Overall increased benthic orbital velocities on average, combined with high variability of benthic orbital velocity likely allow for increased water movement, selecting for corals that may experience partial mortality from breakage or debris strikes more frequently. Increased frequency of partial mortality similarly will select for strategies for increased rates for recovery from partial tissue loss. However the negative relationship with maximum benthic orbital velocity indicates there may be a limit on this relationship, and as benthic orbital velocities exceed these limits the added wave energy may be too stressful for corals to devote energy to accelerated recovery.

Similarly the addition of temperature in the modeling of recovery showed a slight sensitivity by *O. franksi*, increasing model fit compared to looking at recovery with depth alone. This is likely driven by the increased variance of *O. franksi* in the mesophotic environment, and, since temperature served a key player between locations within the shallow and mesophotic designations, likely explains some of the variation in *O. franksi*

seen in each depth environment as well. This added sensitivity is contrasted for *A. lamarcki* which had no particular relationship with any variables added to the depth-only models. Within this depth range, *A. lamarcki* recovery appears unaffected by the physical environment or measured colony variables, even showing a somewhat positive relationship with depth and tissue color recovery.

While there are likely additional factors driving both *O. franksi* recovery and *A. lamarcki* recovery, this analysis highlights a fundamental similarities and differences in the recovery abilities and sensitivities of both species. As both species are important reef-building species across this depth-range, differences in recovery is an important factor in considering resilience and recovery ability of reefs dominated by either species across depth.

Although both species are capable of building reef across all of these depths, analysis of lesion recovery rates in areas considered both shallow and mesophotic has shown that each species behaves distinctly from one another. While both species on average have somewhat different recovery rates on average, significant clustering by the *O. franksi* in the shallow environment and *A. lamarcki* in the deep environment suggest a degree of specialization in each environment. As these observations are for the entire recovery period, the time periods represent the beginning, middle, and end of the complete recovery process, and show consistent increased variability for *O. franksi* throughout the recovery process.

As MCEs continue to be investigated as refugia for stress to coral ecosystems in the long term, understanding lesion recovery as it relates to reef resiliency in both MCEs

and shallow water systems is crucial as each environment faces acute stress events. Areas or species with faster recovery rates will inherently persist in the face of increasing stressors, such as storms, mass bleaching events, or increased storm intensity (Diaz-Pulido et al., 2009; Meesters and Bak, 1993). Furthermore understanding key factors that affect stress recovery ability further provides insight to areas, species, or other factors that lead to increased resilience on a given reef, essential information for reef managers and conservationists.

By nature of these differences, environments in the shallow and mesophotic depths may overall recover from stress events drastically different from one another, even with similar relative species abundances of each of these species. In shallow water environments, a reef with abundant *A. lamarcki* may not be able to recover as well as a mesophotic reef dominated by *A. lamarcki*, with the reverse true for shallow and mesophotic areas composed primarily of *O. franksi*. In the northern US Virgin Islands, the upper mesophotic is frequently composed of wide expanses of *Orbicella* spp.-dominated reef, however in the wake of increasing stress events such as bleaching and severe storms, these reefs may be unable to recover and over time see significant declines.

This is of particular concern in the face of rising global ocean temperatures and increased frequency of bleaching events across depth (Hoegh-Guldberg et al. 2007, Hughes et al. 2003). In the US Virgin Islands, MCEs have overall lower bleaching thresholds, putting them at increased risk for bleaching events as the ocean continues to warm (Smith et al. 2016). With tissue recovery following bleaching events slowed by

both depth and warmer ocean temperatures, areas with *O. franksi* will likely be limited by their recovery ability. Over the long term, this may lead to decreased stress recovery, and, in areas of increased acute stress events, a loss of *O. franksi* in MCEs. Similarly for *A. lamarcki*, increased stress events in shallow water systems, such as intense storms, may challenge the adaptable nature of each individual across depth, further pushing *A. lamarcki* as depth-specialists more than depth generalists.

Investigating stress response and tissue recovery of scleractinian corals is essential in understanding and preservation of coral reef ecosystems in the long term, in particular in the face of rapidly changing global climate. As chronic stressors to reefs strengthen acute stress events that bring about partial mortality increase in frequency and severity, and as a result tissue recovery continues to increase in importance in the energy budget and prioritization of corals for competition and survival. As MCEs continue to be studied and investigated, understanding key differentiating factors in both the physical environment and the foundational species present will be essential for continued survival.

Bibliography

- Anthony, K. R. N., Connolly, S. R., Hoegh-Guldberg, O. (2007), Bleaching, energetics, and coral mortality risk: Effects of temperature, light, and sediment regime, *Limnology and Oceanography*, 52, <https://doi.org/10.4319/lo.2007.52.2.0716>
- Anthony, K. R. N., Hoogenboom, M. O., Maynard, J.A., Grottoli, A. G., Middlebrook, R. (2009). Energetics approach to predicting mortality risk from environmental stress: a case study of coral bleaching. *Functional Ecology* 23(3): 539-550. <https://doi.org/10.1111/j.1365-2435.2008.01531.x>
- Appeldoorn, R., Ballantine, D., Bejarano, I., Carlo, M., Nemeth, M., Otero, E., Pagan, F., Ruiz, H., Schizas, N., Sherman, C., Weil, E. (2016). Mesophotic coral ecosystems under anthropogenic stress: a case study at Ponce, Puerto Rico. *Coral Reefs* 35: 63. <https://doi.org/10.1007/s00338-015-1360-5>
- Bak, R. P. M., & Steward-Van Es, Y. (1980). Regeneration of Superficial Damage in the Scleractinian Corals *Agaricia Agaricites F. Purpurea* and *Porites Astreoides*. *Bulletin of Marine Science*, 30(4), 883–887. Retrieved from <http://www.ingentaconnect.com/content/umrsmas/bullmar/1980/00000030/00000004/art00010+>
- Booij, N., R.C. Ris and L.H. Holthuijsen, 1999, A third-generation wave model for coastal regions, Part I, Model description and validation, *J. Geophys. Res.* C4, 104, 7649-7666.
- Brandtneris, V. W., Brandt, M., Glynn, P. W., Gyory, J., & Smith, T. B. (2016). Seasonal Variability in Calorimetric Energy Content of Two Caribbean Mesophotic Corals. *PLoS ONE*, 11(4), 1–19. <https://doi.org/10.17605/OSF.IO/TC7KZ>
- Bongaerts, P., Ridgway, T., Sampayo, E. M., & Hoegh-Guldberg, O. (2010). Assessing the “deep reef refugia” hypothesis: focus on Caribbean reefs. *Coral Reefs*, 29(2), 309–327.
- Bongaerts, P., Frade, P. R., Ogier, J. J., Hay, K. B., Van Bleijswijk, J., Englebert, N., ... Hoegh-Guldberg, O. (2013). Sharing the slope: Depth partitioning of agariciid corals and associated Symbiodinium across shallow and mesophotic habitats (2-60 m) on a Caribbean reef. *BMC Evolutionary Biology*, 13(1). <https://doi.org/10.1186/1471-2148-13-205>
- Bongaerts, P., Frade, P. R., Hay, K. B., Englebert, N., Latijnhouwers, K. R. W., Bak, R. P. M., ... Hoegh-Guldberg, O. (2015). Deep down on a Caribbean reef: Lower mesophotic depths harbor a specialized coral-endosymbiont community. *Scientific Reports*, 5. <https://doi.org/10.1038/srep07652>

- Cairns, S. D. (1982). Stony corals (Cnidaria: Hydrozoa, Scleractinia) of Carrie Bow Cay, Belize. *Smithsonian Contributions To the Marine Sciences*, 271–302. <https://doi.org/10.1002/iroh.19840690135>
- Carilli, J., Donner, S. D., & Hartmann, A. C. (2012). Historical temperature variability affects coral response to heat stress. *PLoS ONE*, 7(3), 1–9. <https://doi.org/10.1371/journal.pone.0034418>
- Counsell, C. W. W., Johnston, E. C., & Sale, T. L. (2019). Colony size and depth affect wound repair in a branching coral. *Marine Biology*, (October). <https://doi.org/10.1007/s00227-019-3601-6>
- Darling, E. S., Alvarez-Filip, L., Oliver, T. A., McClanahan, T. R., & Côté, I. M. (2012). Evaluating life-history strategies of reef corals from species traits. *Ecology Letters*, 15(12), 1378–1386. <https://doi.org/10.1111/j.1461-0248.2012.01861.x>
- Diaz-Pulido, G., McCook, L. J., Dove, S., Berkelmans, R., Roff, G., Kline, D. I., ... Hoegh-Guldberg, O. (2009). Doom and Boom on a Resilient Reef: Climate Change, Algal Overgrowth and Coral Recovery. *PLOS ONE*, 4(4), e5239. Retrieved from <https://doi.org/10.1371/journal.pone.0005239>
- Dikou, A., & Van Woesik, R. (2006). Partial colony mortality reflects coral community dynamics: A fringing reef study near a small river in Okinawa, Japan. *Marine Pollution Bulletin*, 52(3), 269–280. <https://doi.org/10.1016/j.marpolbul.2005.08.021>
- Dustan, P. (1975). Growth and form in the reef-building coral *Montastrea annularis*. *Marine Biology*, 33(2), 101–107. <https://doi.org/10.1007/BF00390714>
- EM, B., JR, F., Kaufman, L., & Rotjan R D. (2017). Temperature and symbiosis affect lesion recovery in experimentally wounded, facultatively symbiotic temperate corals . *Marine Ecology Progress Series*, 570, 87–99. Retrieved from <https://www.int-res.com/abstracts/meps/v570/p87-99>
- Emanuel, K. (2005). Increasing destructiveness of tropical cyclones over the past 30 years. *Nature*, 436(7051), 686–688. <https://doi.org/10.1038/nature03906>
- Fabricius, K. E. (2005). Effects of terrestrial runoff on the ecology of corals and coral reefs: Review and synthesis. *Marine Pollution Bulletin*, 50(2), 125–146. <https://doi.org/10.1016/j.marpolbul.2004.11.028>
- Fine, M., Oren, U., & Loya, Y. (2002). Bleaching effect on regeneration and resource translocation in the coral *Oculina patagonica*. *Marine Ecology Progress Series*, 234, 119–125

- Fisher, E. M., Fauth, J. E., Hallock, P., & Woodley, C. M. (2007). Lesion regeneration rates in reef-building corals *Montastraea* spp. as indicators of colony condition. *Marine Ecology Progress Series*, 339(1994), 61–71.
<https://doi.org/10.3354/meps339061>
- Glynn, P. W. (1996). Coral reef bleaching: facts, hypotheses and implications. *Global Change Biology*, 2: 495–509. doi:10.1111/j.1365-2486.1996.tb00063.x
- Goulet, T. L., Lucas, M. Q., & Schizas, N. V. (2019). Symbiodiniaceae Genetic Diversity and Symbioses with Hosts from Shallow to Mesophotic Coral Ecosystems.
<https://doi.org/10.1007/978-3-319-92735-0>
- Groves SH, Holstein DM, Enochs IC, Kolodziej G, Manzello DP, Brandt ME, Smith TB (2018) Growth rates of *Porites astreoides* and *Orbicella franksi* in mesophotic habitats surrounding St. Thomas, US Virgin Islands. *Coral Reefs*.
- Hammerman, N.M., Rivera-Vicens, R.E., Galaska, M.P., Weil, E., Appeldoorn, R. S., Alfaro, M., Schizas, N. V. (2018). Population connectivity of the plating coral *Agaricia lamarcki* from southwest Puerto Rico. *Coral Reefs* 37: 183.
<https://doi.org/10.1007/s00338-017-1646-x>
- Hall, V. R. (1997). Interspecific differences in the regeneration of artificial injuries on scleractinian corals. *Journal of Experimental Marine Biology and Ecology*, 212(1), 9–23. [https://doi.org/https://doi.org/10.1016/S0022-0981\(96\)02760-8](https://doi.org/https://doi.org/10.1016/S0022-0981(96)02760-8)
- Henry, L.-A., & Hart, M. (2005). Regeneration from Injury and Resource Allocation in Sponges and Corals – a Review. *International Review of Hydrobiology*, 90(2), 125–158. <https://doi.org/10.1002/iroh.200410759>
- Hinderstein, L. M., Martinez, F. A., Dowgiallo, Á. M. J., Puglise, K. A., Marr, J. C. A., Pyle, R. L., ... Appeldoorn, R. (2010). Theme section on Mesophotic Coral Ecosystems: Characterization, Ecology, and Management’ a scientific workshop was held in Jupiter, Florida, to identify critical research and resource management needs for mesophotic coral ecosystems. *Coral Reefs*, 29, 247–251.
<https://doi.org/10.1007/s00338-010-0614-5>
- Hoegh-Guldberg, O., Mumby, P. J., Hooten, A. J., Steneck, R. S., Greenfield, P., Gomez, E., ... Hatziolos, M. E. (2007). Coral Reefs Under Rapid Climate Change and Ocean Acidification. *Science*, 318(5857), 1737–1742.
<https://doi.org/10.1126/science.1152509>

- Hoeksema, B.W., Bongaerts, P. & Baldwin, C.C. (2017). High coral cover at lower mesophotic depths: a dense *Agaricia* community at the leeward side of Curaçao, Dutch Caribbean. *Marine Biodiversity* 47: 67. <https://doi.org/10.1007/s12526-015-0431-8>
- Iglesias-prieto, R., & Schmidt, G. W. (2014). Community dynamics and physiology of *Symbiodinium* spp . before , during , and after a coral bleaching event, (MAY). <https://doi.org/10.4319/lo.2014.59.3.0788>
- Kahng, S.E., Garcia-Sais, J.R., Spalding, H.L., Brokovich, E., Wagner, D., Weil, E., Hinderstein, L., Toonen, R. J. (2010). Community ecology of mesophotic coral reef ecosystems. *Coral Reefs* 29: 255. <https://doi.org/10.1007/s00338-010-0593-6>
- Knutson TR, Sirutis JJ, Zhao M, Tuleya RE, Bender M, Vecchi GA, Villarini G, Chavas D (2015) Global projections of intense tropical cyclone activity for the late twenty-first century from dynamical downscaling of CMIP5/RCP4.5 scenarios. *Journal of Climate* 28:7203-7224
- Kramarsky-Winter, E., & Loya, Y. (2000). Tissue regeneration in the coral *Fungia granulosa*: the effect of extrinsic and intrinsic factors. *Marine Biology*, 867–873. Retrieved from <http://link.springer.com/article/10.1007/s002270000416>
- LaJeunesse, T. C., Pettay, D. T., Sampayo, E. M., Phongsuwan, N., Brown, B., Obura, D. O., ... Fitt, W. K. (2010). Long-standing environmental conditions, geographic isolation and host-symbiont specificity influence the relative ecological dominance and genetic diversification of coral endosymbionts in the genus *Symbiodinium*. *Journal of Biogeography*, 37, 785–800. <https://doi.org/10.1111/j.>
- LaJeunesse, T. C., J. E. Parkinson, P. W. Gabrielson, H. J. Jeong, J. D. Reimer, C. R. Woolstra, and S. R. Santos. (2018). Systematic revision of Symbiodiniaceae highlights the antiquity and diversity of coral endosymbionts. *Current Biology* 28:2570-2580.e2576.
- Laverick, J. H., & Rogers, A. D. (2018). Experimental evidence for reduced mortality of *Agaricia lamarcki* on a mesophotic reef. *Marine environmental research*, 134, 37-43.
- Levitan, D., Boudreau, W., Jara, J., & Knowlton, N. (2014). Long-term reduced spawning in *Orbicella* coral species due to temperature stress. *Marine Ecology Progress Series*, 515, 1–10. <https://doi.org/10.3354/meps11063>
- Lesser, Michael P., Slattery, Marc, Leichter, James J. (2009). Ecology of mesophotic coral reefs. *Journal of Experimental Marine Biology and Ecology*, 375(1-2), 1-8

- Lopez, J. V., Kersanach, R., Rehner, S. A., & Knowlton, N. (1999). Molecular Determination of Species Boundaries in Corals: Genetic Analysis of the *Montastraea annularis* Complex Using Amplified Fragment Length Polymorphisms and a Microsatellite Marker. *Biol. Bull.*, 196, 80–93.
- Lugo-Fernández, A., & Gravois, M. (2010). Understanding impacts of tropical storms and hurricanes on submerged bank reefs and coral communities in the northwestern Gulf of Mexico. *Continental Shelf Research*, 30(10–11), 1226–1240. <https://doi.org/10.1016/j.csr.2010.03.014>
- Maltby, L. (1999). Studying stress: the importance of organism-level responses. *Ecological Applications*, 9(2), 431–440. [https://doi.org/10.1890/1051-0761\(1999\)009\[0431:SSTIOO\]2.0.CO;2](https://doi.org/10.1890/1051-0761(1999)009[0431:SSTIOO]2.0.CO;2)
- Mascarelli, P. E., & Bunkley-Williams, L. (1999). An experimental field evaluation of healing in damaged, unbleached and artificially bleached star coral, *Montastraea annularis*. *Bulletin of Marine Science*, 65(2), 577–586. <https://doi.org/10.3354/meps062185>
- Menza, C., Kendall, M., & Hile, S. (2008). The deeper we go the less we know. *Revista de Biología Tropical*, 56(1), 11–24.
- Meesters, E. H., & Bak, R. P. M. (1993). Effects of coral bleaching on tissue regeneration potential and colony survival. *Marine Ecology Progress Series*, 96(2), 189–198. Retrieved from <http://www.jstor.org/sTable/24833544>
- Meesters, E. H., Noordeloos, M., & Bak, R. P. M. (1994). Damage and regeneration: links to growth in the reef-building coral *Montastrea annularis*. *Marine Ecology Progress Series*, 112(1/2), 119–128. Retrieved from <http://www.jstor.org.ezaccess.libraries.psu.edu/sTable/24847643>
- Meesters, E., Wesseling, I., & Bak, R. P. M. (1996). Partial mortality in three species of reef-building corals and the relation with colony morphology. *Bulletin of Marine Science*, 58(3), 838–852.
- Moberg, F., & Folke, C. (1999). Ecological goods and services of coral reef ecosystems. *Ecological Economics*, 29(2), 215–233. [https://doi.org/10.1016/S0921-8009\(99\)00009-9](https://doi.org/10.1016/S0921-8009(99)00009-9)
- Nagelkerken, I., Meesters, E. H., & Bak, R. P. M. (1999). Depth-related variation in regeneration of artificial lesions in the Caribbean corals *Porites astreoides* and *Stephanocoenia michelinii*. *Journal of Experimental Marine Biology and Ecology*, 234(1), 29–39. [https://doi.org/https://doi.org/10.1016/S0022-0981\(98\)00147-6](https://doi.org/https://doi.org/10.1016/S0022-0981(98)00147-6)

- NOAA, (2016). “Coral Laceration Regeneration Assay”. Coral Disease & Health Consortium, Accessed 3/16/2016. https://cdhc.noaa.gov/education/coral_assay.aspx
- Pandolfi, J. M., & Budd, A. F. (2008). Morphology and ecological zonation of Caribbean reef corals: The *Montastraea* “annularis” species complex. *Marine Ecology Progress Series*, 369(Goreau 1959), 89–102. <https://doi.org/10.3354/meps07570>
- Plaisance, L., Caley, M. J., Brainard, R. E., & Knowlton, N. (2011). The diversity of coral reefs: What are we missing? *PLoS ONE*, 6(10). <https://doi.org/10.1371/journal.pone.0025026>
- Rogers, C. S. (1993). Hurricanes and coral reefs: the intermediate disturbance hypothesis revisited. *Coral Reef*, 12, 127–137. <https://doi.org/10.1007/BF00304729>
- Ruiz-Diaz, C. P., Toledo-Hernandez, C., Mercado-Molina, A. E., Pérez, M. E., & Sabat, A. M. (2016). The role of coral colony health state in the recovery of lesions. *PeerJ*, 2016(1), 1–13. <https://doi.org/10.7717/peerj.1531>
- Sabine, A. M., Smith, T. B., Williams, D. E., & Brandt, M. E. (2015). Environmental conditions influence tissue regeneration rates in scleractinian corals. *Marine Pollution Bulletin*, 95(1), 253–264. doi:10.1016/j.marpolbul.2015.04.006
- Shirur, K. P., Jackson, C. R., & Goulet, T. L. (2016). Lesion recovery and the bacterial microbiome in two Caribbean gorgonian corals. *Marine Biology*. <https://doi.org/10.1007/s00227-016-3008-6>
- Slattery, M., Lesser, M. P., Brazeau, D., Stokes, M. D., & Leichter, J. J. (2011). Connectivity and stability of mesophotic coral reefs. *Journal of Experimental Marine Biology and Ecology*, 408(1), 32–41. <https://doi.org/https://doi.org/10.1016/j.jembe.2011.07.024>
- Smith, T. B., Blondeau, J., Nemeth, R. S., Pittman, S. J., Calnan, J. M., Kadison, E., & Gass, J. (2010). Benthic structure and cryptic mortality in a Caribbean mesophotic coral reef bank system, the Hind Bank Marine Conservation District, U.S. Virgin Islands. *Coral Reefs*, 29(2), 289–308. <https://doi.org/10.1007/s00338-009-0575-8>
- Smith, T. B., M. E. Brandt, V. W. Brandtneris, R. S. Ennis, S. H. Groves, S. Habtes, D. M. Holstein, E. Kadison, and R. S. Nemeth. (2019a). Disturbance in Mesophotic Coral Ecosystems and Linkages to Conservation and Management.in Y. Loya, K. A. Puglise, and T. Bridge, editors. *Coral Reefs of the World: Mesophotic Coral Ecosystems*. Springer.

- Smith, T. B., M. E. Brandt, V. W. Brandtneris, R. S. Ennis, S. H. Groves, S. Habtes, D. M. Holstein, E. Kadison, and R. S. Nemeth. (2019b). The United States Virgin Islands. In Y. Loya, K. A. Puglise, and T. Bridge, editors. *Coral Reefs of the World: Mesophotic Coral Ecosystems*. Springer.
- Smith, T. B., Brandtneris, V. W., Canals, M., Brandt, M. E., Martens, J., Brewer, R. S., ... Holstein, D. M. (2016a). Potential Structuring Forces on a Shelf Edge Upper Mesophotic Coral Ecosystem in the US Virgin Islands. *Frontiers in Marine Science*, 3(June). <https://doi.org/10.3389/fmars.2016.00115>
- Smith TB, Ennis RS, Kadison E, Weinstein DW, Jossart J, Gyory J, Henderson L (2015) The United States Virgin Islands Territorial Coral Reef Monitoring Program. Year 15 Annual Report. Version 1 288 pp
- Smith, T. B., Gyory, J., Brandt, M. E., & Miller, W. J. (2016b). Caribbean mesophotic coral ecosystems are unlikely climate change refugia, 1–10. <https://doi.org/10.1111/gcb.13175>
- Smith T.B., Holstein D.M., Ennis R.S. (2019) Disturbance in Mesophotic Coral Ecosystems and Linkages to Conservation and Management. In: Loya Y., Puglise K., Bridge T. (eds) *Mesophotic Coral Ecosystems*. *Coral Reefs of the World*, vol 12. Springer, Cham
- Studivan, M. S., Milstein, G., & Voss, J. D. (2019). *Montastraea cavernosa* corallite structure demonstrates distinct morphotypes across shallow and mesophotic depth zones in the Gulf of Mexico. *PLoS ONE*, 14(3), 1–21. <https://doi.org/10.1371/journal.pone.0203732>
- Todd, P. A. (2008). Morphological plasticity in scleractinian corals. *Biological Reviews*, 83(3), 315–337. <https://doi.org/10.1111/j.1469-185X.2008.00045.x>
- Weil, E., & Knowlton, N. (1989). a Multi-Character Analysis of the Caribbean Coral *Montastraea Annularis*. *Bulletin of Marine Science*, 55(September), 151–175.
- Weinstein DK, Sharifi A, Klaus JS, Smith TB, Giri SJ, Helmle KP (2016). Coral growth, bioerosion, and secondary accretion of living orbicellid corals from mesophotic reefs in the US Virgin Islands. *Mar Ecol Prog Ser* 559:45-63. <https://doi.org/10.3354/meps11883>